Newsletter of the Climate Variability and Predictability Programme (CLIVAR)

Exchanges

No. 23 (Vol. 7, No. 1) March 2002

Special issue on: Tropical-Extratropical Interactions

Latest CLIVAR News

- The First CLIVAR Science Conference June 21-25, 2004 in Baltimore, USA. Bookmark this important meeting in your calendars.
- Southern Ocean Panel in place.
  Visit: www.clivar.org
  -> Organization
  -> Southern Ocean
- Continously growing interest for CLIVAR Exchanges, currently we have about 1600 subscriptions for our newsletter.
- New search function and alphabetical index of the CLIVAR Website. It is now easier to navigate around.

Visit our news page:
http://www.clivar.org/recent/

CLIVAR is an international research programme dealing with climate variability and predictability on time-scales from months to decades.

CLIVAR is a component of the World Climate Research Programme (WCRP).

Euro-Mediterranean rainfall variability and ENSO

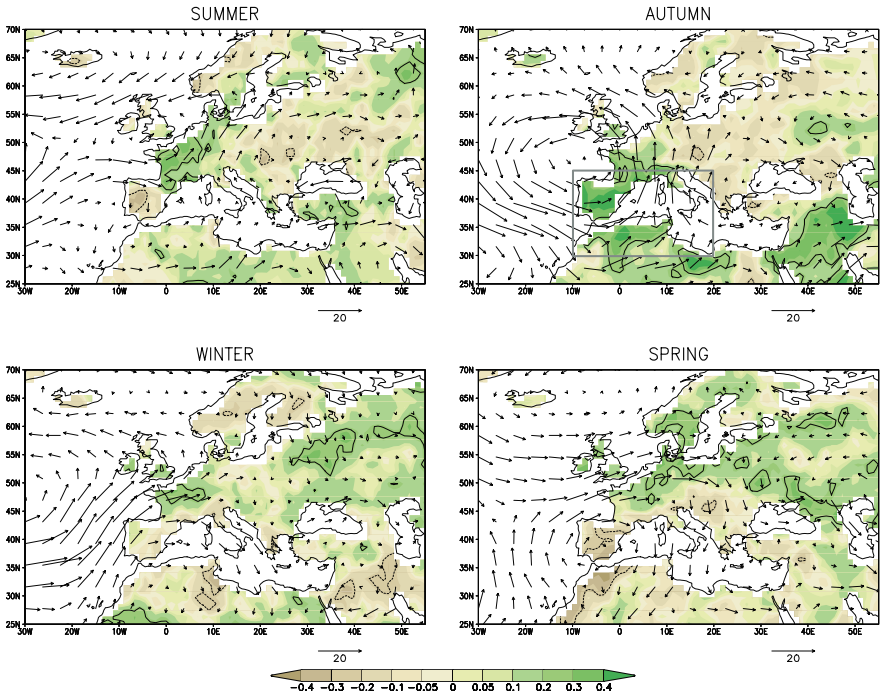

Figure 1 from paper '*Euro-Mediterranean rainfall variability and ENSO*' by A. Mariotti et al.:
Seasonal correlation of rainfall (CRU) in the Euro-Mediterranean region with the Niño3.4 index for the period 1948-1996 (shaded). The seasonal regression of vertically integrated moisture flux (NCEP) with the Niño3.4 index for the period 1948-98 is also plotted (vectors). Correlation coefficients enclosed by contours are statistically significant at the 95% level. The grey box encloses the region considered to compute western Mediterranean area-averages.
The paper appears on page 3.

Call for Contributions

We would like to invite the CLIVAR community to submit articles to CLIVAR Exchanges for the next issue.The overarching topic will be on **science related to the Pacific**, e.g., all aspects of ENSO, papers relevant to projects like PACS, EPIC, KESS, etc.) **The deadline for this issue is May 1, 2002.**
Guidelines for the submission of papers for CLIVAR Exchanges can be found under: http://www.clivar.org/publications/exchanges/guidel.htm

Editorial

Dear CLIVAR community,

Welcome to the first issue of CLIVAR Exchanges in 2002. We are starting the 7th year of our newsletter with a new layout but with the same interesting science content. In this edition we have focused on Tropical-extra-tropical interactions. We hope that you will be pleased with both the appearance and the content.

The first three months of 2002 have already been busy ones for CLIVAR with meetings of some of our working groups, preparations for the annual presentation to the WCRP's Joint Scientific Committee and preparations for the 11th CLIVAR SSG in Xi'an, China in May.

CLIVAR's organisational structure is now almost complete following the formation of two new panels. One covers the Pacific sector and it met for the first time in February 2002. It will play a key role in linking together implementation not just relating to ENSO, but also for other Pacific-area phenomena with timescales from interannual to decadal and longer. The Pacific panel has already caught the attention of the North Pacific Marine Organisation (PICES). PICES aims to "Advance scientific knowledge about the ocean environment, global weather and climate change, living resources and their ecosystems, and the impacts of human activities". With that in mind a joint (PICES/CLIVAR) workshop is planned in October 2002. (http://www.pices.ios.bc.ca). In the Pacific we are developing an exciting international coordinated effort to better understand climate. It will potentially benefit a huge part of the earth's population by giving improved climate predictions within the next decade. We will report about the Pacific Panel meeting in the next issue.

The other panel covers the Southern Ocean sector and is a joint effort with our partner programme in the World Climate Research Programme CliC (Climate and Cryosphere). The Southern Ocean area poses huge logistical difficulties for the establishment of sustained climate observations. Yet it is of huge importance because of the role of the Antarctic circulation acting as both a link between the world's oceans and a driver of climate variability. Thus, a better understanding of high latitude processes and the variability in the Southern Ocean area will be beneficial for many aspects of CLIVAR. The CLIVAR Southern Ocean Panel will hold its first meeting in Hobart, Australia in March. It will meet in parallel with the International Argo Science Team that is overseeing the implementation of the Argo global array of profiling floats. Argo will play a key role, in the remote Southern Ocean and so the close links between these two panels is both appropriate and timely.

Since the CLIVAR Pacific panel met in Honolulu back-to-back with the AGU/ASLO Ocean Sciences meeting, there was a good opportunity for CLIVAR scientists and ICPO staff to meet informally and to participate in the many CLIVAR-related sessions at the meeting. A major activity was a 3-day conference session on the North Atlantic climate. It was remarkable in that meeting to see how much we have learned over the past decade about the decadal variability of that ocean and its links to atmospheric forcing. There was also an opportunity for a meeting of CLIVAR and ocean carbon researchers to assess progress towards a global re-survey of ocean carbon inventories. The outlook is very promising and will be reported on in a future newsletter.

Recent meetings of CLIVAR's two modelling panels, the Working Group on Seasonal to Interannual Prediction (WGSIP) and the JSC/CLIVAR Working Group on Coupled Modelling (WGCM), have documented progress in this key area. Summaries can be found on pages 25-26 of this issue.

Looking forward, we are expecting further progress in the VAMOS programme that will develop plans for a North American Monsoon Experiment (NAME) and a strategy for a project in the eastern equatorial Pacific. The VAMOS panel will meet in mid-March.

We should not give the impression that CLIVAR is just meetings. A visit to the CLIVAR web pages will show the rapid pace of implementation. This is most visible in the oceans where new initiatives will result in monitoring of the Atlantic thermohaline circulation, a moored array in the Indonesian Throughflow, a comprehensive monitoring of the Gulf Stream between Bermuda and the USA, the reoccupation of many hydrographic lines previously occupied during WOCE. The Argo array of profiling floats already delivers 1/3 of the number of profiles that comes from XBTs and the array is expanding very rapidly. Neither should we overlook the satellite observations that will come from an extension of the Topex-Poseidon mission, from Jason-1 and from the launch of ENVISAT.

Beyond 2002, the CLIVAR International Science Conference now has a firm venue and timing. These are now set for June, 21-25, 2004 in Baltimore, USA. Please mark this on your calendars. The scope and format of this first large science conference reviewing the first years of the CLIVAR programme is currently being defined by the organising committee under its chairman Professor Lennart Bengtsson.

John Gould and Andreas Villwock

Euro-Mediterranean rainfall variability and ENSO

A. Mariotti[1], N. Zeng[2] and K.-M. Lau[3]

[1]ENEA, Climate Section, Rome, Italy
currently visiting: U. Maryland, ESSIC, College Park, MD, USA
annarita.mariotti@casaccia.enea.it

[2]U. Maryland, Dept. of Meteorology and ESSIC College Park, MD, USA

[3]NASA-Goddard Space Flight Center, Greenbelt, MD, USA

It has long been a matter of debate whether and how the El Niño-Southern Oscillation (ENSO) warm and cold extremes influence Euro-Mediterranean rainfall. In fact while the impact of ENSO on tropical climate is well-established, the response in the North-Atlantic European region is far less understood. Since the early observational studies by Ropelewsky and Halpert (1987) and Kiladis and Diaz (1989) some anomalous rainfall was documented in the region at particular stages of the ENSO events, but results were overall inconclusive. Later works have pointed to significant ENSO related climate anomalies mostly during winter and spring (Fraedrich and Muller, 1992; Rodo et al., 1997, Moron and Ward, 1998; van Oldenborgh et al., 2000). Dong et al. (2000) successfully simulated the winter circulation anomalies observed in the Atlantic sector during the 97/98- 98/99 ENSO cycle and showed how these were primarily forced by ENSO-related SST anomalies in the Pacific ocean. Pozo-Vasquez et al. (2001) and Cassou et al. (2001a,b) suggest that ENSO influences the North Atlantic/European region more strongly during cold events and indicate that possible mechanisms may involve an extention of the effects of the PNA pattern towards Europe and the influence of ENSO-related tropical Atlantic SST anomalies. Merkel and Latif (2002), by means of high resolution AGCM simulations, show that in winter El Niño events have a significant impact over Europe on both the seasonal climatic means and the wave activity.

In this short contribution, which summarizes the results to appear shortly in Mariotti et al. (2002), we report new observational evidence regarding the relation between ENSO and the interannual variability of rainfall in the Euro-Mediterranean sector, evidencing, in particular, spatially coherent correlation patterns and their seasonal variations.

1. Results

Figure 1 (page 1) presents the correlation between CRU (Climatic Research Unit, U. East Anglia, UK) rainfall in the Euro-Mediterranean region and the Niño3.4 index for the four standard seasons of the year during the period 1948-1996 (CRU is a land-only rain-gauge based gridded high resolution precipitation dataset; New et al., 2000). Spatially coherent patterns are found in central and eastern Europe where the correlation is negative in autumn and positive during winter and spring. In western Europe and the Mediterranean region the correlation is positive in autumn and negative in spring. The correlation coefficients derived using rainfall from NCEP/NCAR re-analyses (NCEP hereafter; Kalnay et al., 1996), ECMWF re-analyses (ERA hereafter; Gibson et al., 1997), and CMAP (these are gauge-satellite merged analyses of precipitation; Xie et al., 1996) are broadly consistent with those from CRU for the period during which they are available and show the above mentioned spatially coherent patterns also extending to the nearby Atlantic ocean and the Mediterranean sea (not shown). The regression of NCEP data with Niño3.4 indicates a seasonally changing anomalous moisture flux in association with the observed rainfall anomalies (Figure 1, page 1): in autumn an anomalous cyclonic circulation brings enhanced moisture from the Atlantic to the western Mediterranean region; this flow turns north at about 20E, separating positive rainfall anomalies in the western Mediterranean and negative anomalies in the eastern Mediterranean. Anomalous moisture coming from the Arabian Sea brings more rain to Middle East regions toward the Caspian Sea. In winter and spring, a warm event causes anomalous moisture from the subtropical Atlantic to be channeled away from western Europe and toward higher latitudes where positive rainfall anomalies are found.

The ENSO composite analysis of rainfall anomalies (both CRU and NCEP) in the Euro-Mediterranean region (not shown) is in agreement with the results of the correlation maps in Figure 1 (page 1) . The analysis further indicates that the autumn correlation is mostly due to the autumn season of the "year 0", immediately before the mature phase of ENSO, while the winter and spring signals come mostly from the "year +1", during and after the mature phase. We now focus on the characteristics of the western Mediterranean rainfall where there is the strongest ENSO signal in the studied land domain (the area is defined by the box in Fig. 1). In Figure 2 a we show the correlation between 3-month mean rainfall for this region and the Niño3.4 index. All 4 datasets show a change of this correlation from positive in autumn to negative in spring.

Western Mediterranean autumn and spring rainfall anomalies correlate significantly with global SST anomalies (SST are from the GISST dataset; Rayner et al., 1997) giving spatially coherent patterns which, especially in the Eastern Pacific, are very similar to those invoked by a typical ENSO event (see Figure 3). ENSO-like correlation is also found in the Indian Ocean and South-East Pacific but only in autumn; in spring, correlation is significant in the Western Pacific along the coast

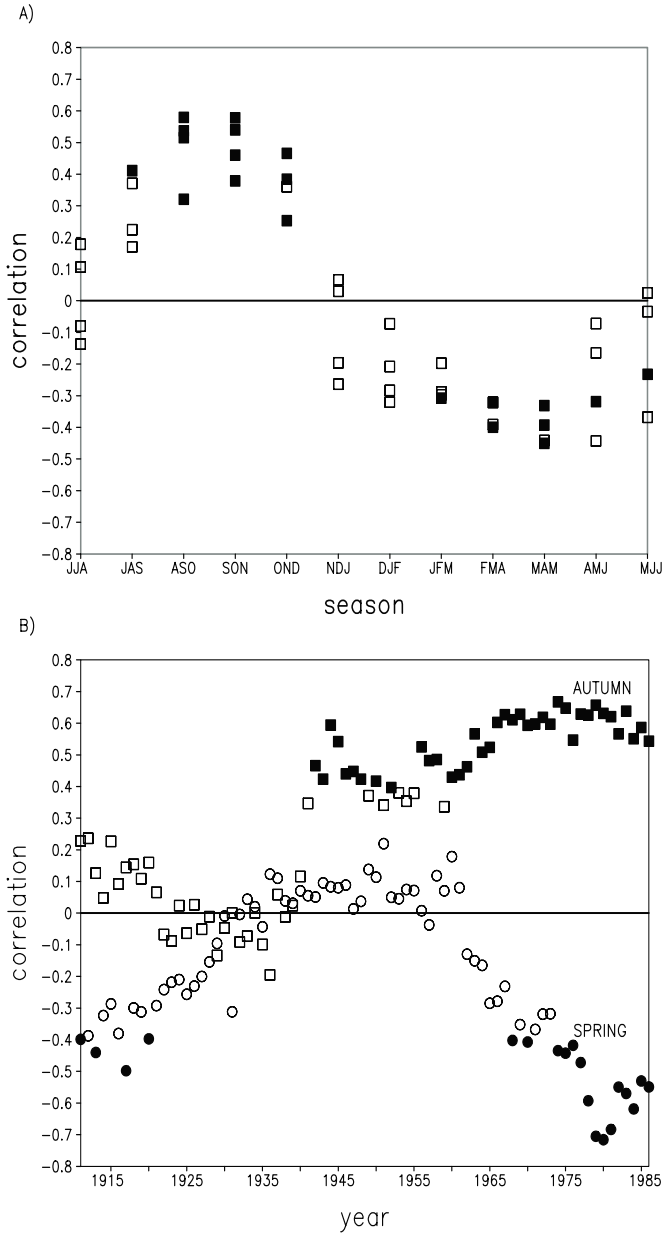

Fig. 2: Correlation between western Mediterranean rainfall and the Niño3.4 index for various 3-month means and datasets (full symbols are for values which are significant at the 95% level, empty symbols are for non-significant values).
a): Seasonal correlation for various datasets (the periods considered are 1948-96 for CRU, 48-98 for NCEP, 79-93 for ERA and 79-97 for CMAP; CRU is land-only).
b): Autumn (SON, squares) and spring (MAM, circles) correlation for CRU rainfall. Each value refers to the correlation for the 20-year window centered at the symbol.

of South-East Asia. In the Atlantic, areas of significant correlation are mostly found in the sub-tropics where, close to the western Mediterranean, values are negative for both seasons.

The relation between Euro-Mediterranean rainfall and ENSO has changed over the decades during the 20th century. Figure 2b shows the correlation between the Niño3.4 index and western Mediterranean rainfall for a 20-year window sliding from 1910 to 1986. Significant positive values are found for the autumn season starting from the early 1940s. For spring instead, significant positive values are only found early in the century and after the late 1960s.

2. Concluding remarks

The observational results summarized here show that there exists a significant influence of ENSO on rainfall in regions of the Euro-Mediterranean sector with seasonally changing characteristics. In addition to an ENSO-Europe connection in the spring, as noted previously, we also found significant correlation in the autumn. Although absolute anomalies are not large compared to tropical regions, the impact is relevant especially for the regions around the Mediterranean where rainfall can be scarce. For the western Mediterranean we show that ENSO events affect rainfall in an opposite manner during the autumn and the spring seasons immediately before and after the mature phase of an event. In central and eastern Europe, positive anomalies are found in winter and spring during and immediately after the mature phase. A preliminary analysis does not support any clear relationship between the amplitude of the rainfall anomalies in the Euro-Mediterranean sector and the strength of the ENSO events.

The rainfall anomalies in the various seasons are accompanied by an anomalous atmospheric circulation and moisture transport extending from the sub-tropical Atlantic Ocean into the Euro-Mediterranean region. In spring and autumn ENSO-like global SST anomalies are significantly correlated with western Mediterranean rainfall anomalies. However, the mechanisms of how these SST anomalies exert their influence in the far away Euro-Mediterranean region are poorly known.

The relationship between ENSO and Euro-Mediterranean rainfall has been persistent since the latter half of the 20th century; the lack of significant correlation we find in the period 1925-1940 has also characterized ENSO teleconnections in other parts of the globe (for example Hu and Feng, 2001) and may be related to the weaker ENSO activity during this period (Urban et al., 2001).

3. Acknowledgments

We wish to thank all those who have provided the data used for this work. This work was partly supported by the Italian Ministry for Environment (Accordo di Programma ENEA-Ministero Ambiente, Scheda 2.4), NSF grant ATM-0196210 and NASA Global Modeling and Analysis Program, Earth Science Enterprise.

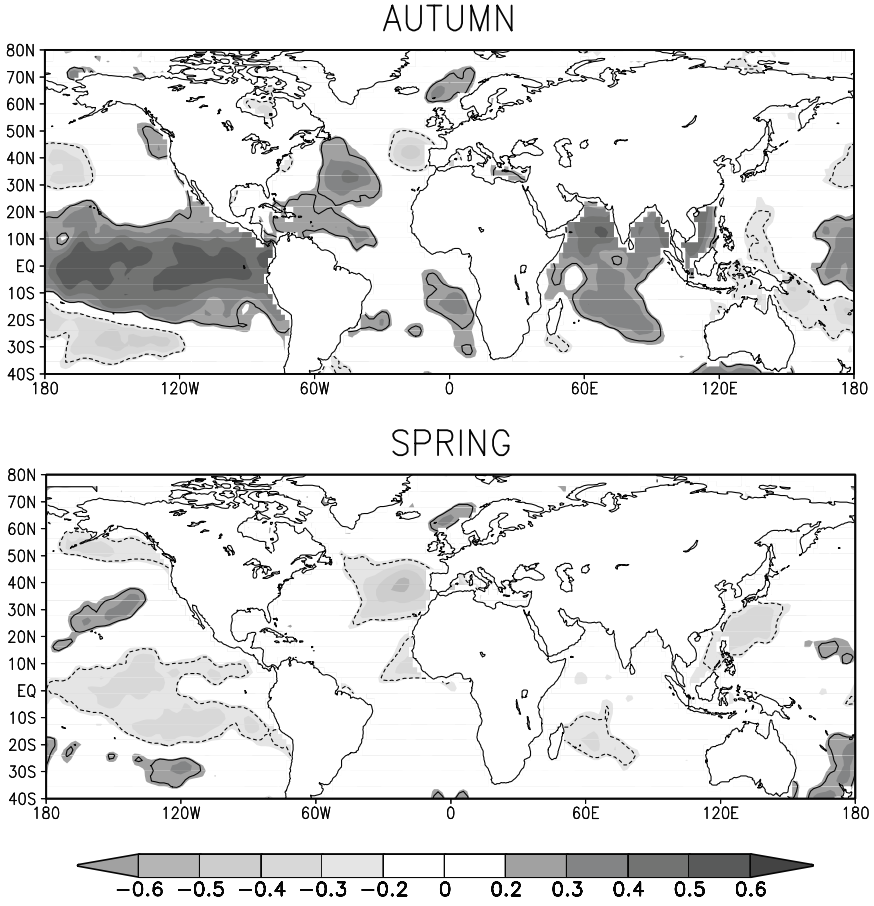

Fig. 3: Correlation between western Mediterranean rainfall and global SST for autumn (SON) and spring (MAM). Rainfall is from CRU (land-only) while SST is from the GISST dataset; the correlation is relative to the period 1948-1996. Values enclosed by contours are statistically significant at the 95% level.

References

Cassou, C., and L. Terray, 2001: Dual Influence of Atlantic and Pacific SST anomalies on the North Atlantic/ Europe Winter Climate. *Geophys. Res. Lett.*, **28**, 3195-3198.

Cassou, C., and L. Terray, 2001: Oceanic forcing of the wintertime low-frequency atmospheric variability in the North Atlantic European Sector: a study with the Arpege model. *J. Climate*, **14**, 4266-4291.

Dong, B.-W., R.T. Sutton, S.P. Jewson, A. O'Neill, and J.M. Slingo, 2000: Predictable winter climate in the North Atlantic sector during the 1997-1999 ENSO cycle. *Geophys. Res. Lett.*, **27**, 985-988.

Fraedrich, K., and K. Müller, 1992: Climate anomalies in Europe associated with ENSO extremes. *Int. J. Climat.*, **12**, 25-31.

Hu, Q., and S. Feng, 2001: Variations of teleconnections of ENSO and interannual variation in summer rainfall in the Central United States, *J. Climate*, **14**, 2469-2480.

Gibson, J.K., P. Kallberg, S. Uppala, A. Hernandez, A. Nomura, and E. Serrano, 1997: ECMWF Re-Analysis Project Report Series: 1. ERA description, *ECMWF, Reading, UK*, 66pp.

Kalnay, E., M, Kanamitsu, R. Kistler, W. Collins, D. Deaven, L. Gandin, M. Iredell, S. Saha, G. White, J. Woollen, Y. Zhu, M. Chelliah, W. Ebisuzaki, W. Higgins, J. Janowiak, K.C. Mo, C. Ropelewski, J. Wang, A. Leetmaa, R. Reynolds, R. Jenne, and D. Joseph, 1996: The NCEP/NCAR 40-year reanalysis project. *Bull. Amer. Meteor. Soc.*, **77**, 437-471.

Kiladis, G.N., and H.F. Diaz, 1989: Global climatic anomalies associated with extremes in the Southern Oscillation. *J. Climate*, **2**, 1069-1090.

Mariotti, A., N. Zeng, and K.-M. Lau, 2002: Euro-Mediterranean rainfall and ENSO - a seasonally varying relationship. *Geophys. Res. Lett.*, in press.

Merkel, U. and M. Latif, 2002: A high resolution study of the EL Niño impact on the North Atlantic/European sector. *Geophys. Res. Lett.*, in press.

Moron, V., and M.N. Ward, 1998: ENSO teleconnections with climate variability in the european and african sectors. *Weather*, **53**, 287-294.

New, M., M. Hulme, and P.D. Jones, 2000: Representing Twentieth-Century Space-Time Climate Variability. Part II: Development of 1901-96 Monthly Grids of Terrestrial Surface Climate. *J. Climate*, **13**, 2217-2238.

van Oldenborgh, G.J., G. Burgers, and A.K. Tank, 2000: On the El-Niño teleconnection to spring precipitation in Europe. *Int. J. Climat.*, **20**, 565-574.

Pozo-Vasquez, D., M.J. Esteban-Parra, F.S. Rodrigo, and Y. Castro-Diez, 2001: The association between ENSO and winter atmospheric circulation and temperature in the North Atlantic region. *J. Climate*, **14**, 3408-3420.

Rayner, N.A., E.B. Horton, D.E. Parker, C.K. Folland, and R.B. Hackett, 1996: Version 2.2 of the Global sea-Ice and Sea Surface Temperature Data Set, 1903-1994. Climate Research Technical Note No. 74. Hadley Centre for Climate Prediction and Research, Meteorological Office, Bracknell, UK.

Rodo, X., E. Baert, and F.A. Comin, 1997: Variations in seasonal rainfall in southern Europe during present century: relationships with the North Atlantic Oscillation and the El Niño Southern Oscillation. *Clim. Dyn.*, **13**, 275-284.

Ropelewski, C.F., and M.S. Halpert, 1987: Global and regional scale precipitation patterns associated with the El Niño/ Southern Oscillation. *Mon. Wea. Rev.*, **115**, 1606-1626.

Urban, F.E., J.E. Cole, and J.T. Overpeck, 2000: Influence of mean climate change on climate variability from a 155-year tropical Pacific coral record. *Nature*, **407**, 989-993.

Xie, P., and P.A. Arkin, 1996: Analysis of global monthly precipitation using gauge observations, satellite estimates and numerical model predictions. *J. Climate*, **9**, 840-858.

The ENSO impact on the North Atlantic/European sector as simulated by high resolution ECHAM4 experiments

Ute Merkel and Mojib Latif
Max-Planck-Institut für Meteorologie
Hamburg, Germany
merkel@dkrz.de

1. Introduction

In the context of atmospheric teleconnections the El Niño/ Southern Oscillation phenomenon operates as an important factor in generating these teleconnections. Several regions such as Indonesia or Australia exhibit a rather stable ENSO related anomaly signal. The North Atlantic/European (NAE) sector, however, is generally considered to experience almost no detectable influence from the tropical Pacific. On the other hand, there exists both numerical modelling and observational evidence that the well-known interaction between the tropical Pacific and the extratropical North Pacific region may extend into the North Atlantic region and thus also might affect the European continent. Compositing observational data, Fraedrich and Müller (1992) demonstrate a small ENSO impact over Europe during winter. Mariotti et al. (2002) find significant correlations of precipitation with tropical Pacific sea surface temperature (SST) for all seasons in parts of the Euro-Mediterranean sector. Numerical studies with different climate models (Ferranti et al., 1994; Bengtsson et al., 1996) have not yet led to a consensus regarding the sign and amplitude of the NAE response.

2. Model experiments

It is often claimed that high horizontal resolution is a crucial ingredient for a more realistic representation of the interaction between eddies and the mean flow in atmospheric general circulation model (AGCM) experiments. It is therefore hypothesized that increased horizontal resolution may be a step towards more insight into the organization of an ENSO response even in far distant regions such as Europe. A recent study (Merkel and Latif, 2002) seeks to elucidate this aspect by conducting seasonal ensemble integrations with the ECHAM4 model at T106 resolution (~1.1˚x1.1˚). The experiments were restricted to the winter season (DJF). Each ensemble consists of five members which only differ in their initial conditions. In a first ensemble, a "canonical" El Niño SST anomaly pattern is prescribed which has been determined from regressing global observed winter (DJF) Reynolds SST anomalies of 1979-98 onto the corresponding Niño3 DJF timeseries. The ensemble mean of this experiment is analyzed with respect to a similar control ensemble with climatological SST. In order to assess the role of resolution, analogous ensembles were performed at T42 resolution.

3. Results

In the Pacific region, both the T42 and the T106 experiments simulate a seasonal ensemble mean response of sea level pressure characterized by the typical Southern Oscillation signature in the tropics and an intensification of the Aleutian low. Further downstream, at both resolutions the meridional North Atlantic pressure gradient is weakened implying an impact on the North Atlantic Oscillation (see Merkel and Latif, 2002, their Fig. 2). The main difference between both resolutions, however, consists in a downstream extension of the significant response into the European continent at T106 resolution. A comparison between the T106 response over Europe with the El Niño composites found by Fradrich and Müller (1992) reveals a qualitative similarity between both patterns (Fig. 1). In order to shed more light on the successful model reproduction of the Fraedrich and Müller results with our T106 experiments, we analyzed the changes in stormtrack activity since the eddies are considered to play a major role in the signal communication from the Pacific/North America into Europe. The bandpass-filtered (2.5-6 days) 500 hPa geopotential height variance over the North Atlantic is reduced, implying a southward shift of the midlatitude cyclone tracks. This is confirmed by the analysis of the Eady growth rate as a measure of baroclinicity which additionally exhibits clear changes in the Mediterranean region.

4. Summary

It is not possible from such complex model simulations to formulate a causal chain describing explicitly how the tropical Pacific signal is transferred to the NAE sector. However, these experiments provide a useful framework to explore the possible components involved in the organization of extratropical anomalies in the NAE sector. We would like to emphasize that, from our experiments, the role of horizontal resolution is somehow ambivalent. While the T106 model response in the Pacific sector is already well captured by the T42 simulation, the T106 resolution appears crucial for simulating a significant signal which ressembles observational composites in the NAE sector.

Interestingly, the response in the NAE sector of the globally forced experiment could be confirmed by a second experiment where the regression-based SST anomalies were only prescribed in the tropical Pacific. This leads us to the conclusion that the tropical Pacific is the main modulator of European climate. A similar La Niña-type ensemble has also been conducted in order to assess the symmetry of the atmospheric response with respect to the anomalous oceanic forcing. A significant response was found even in the NAE sector with close

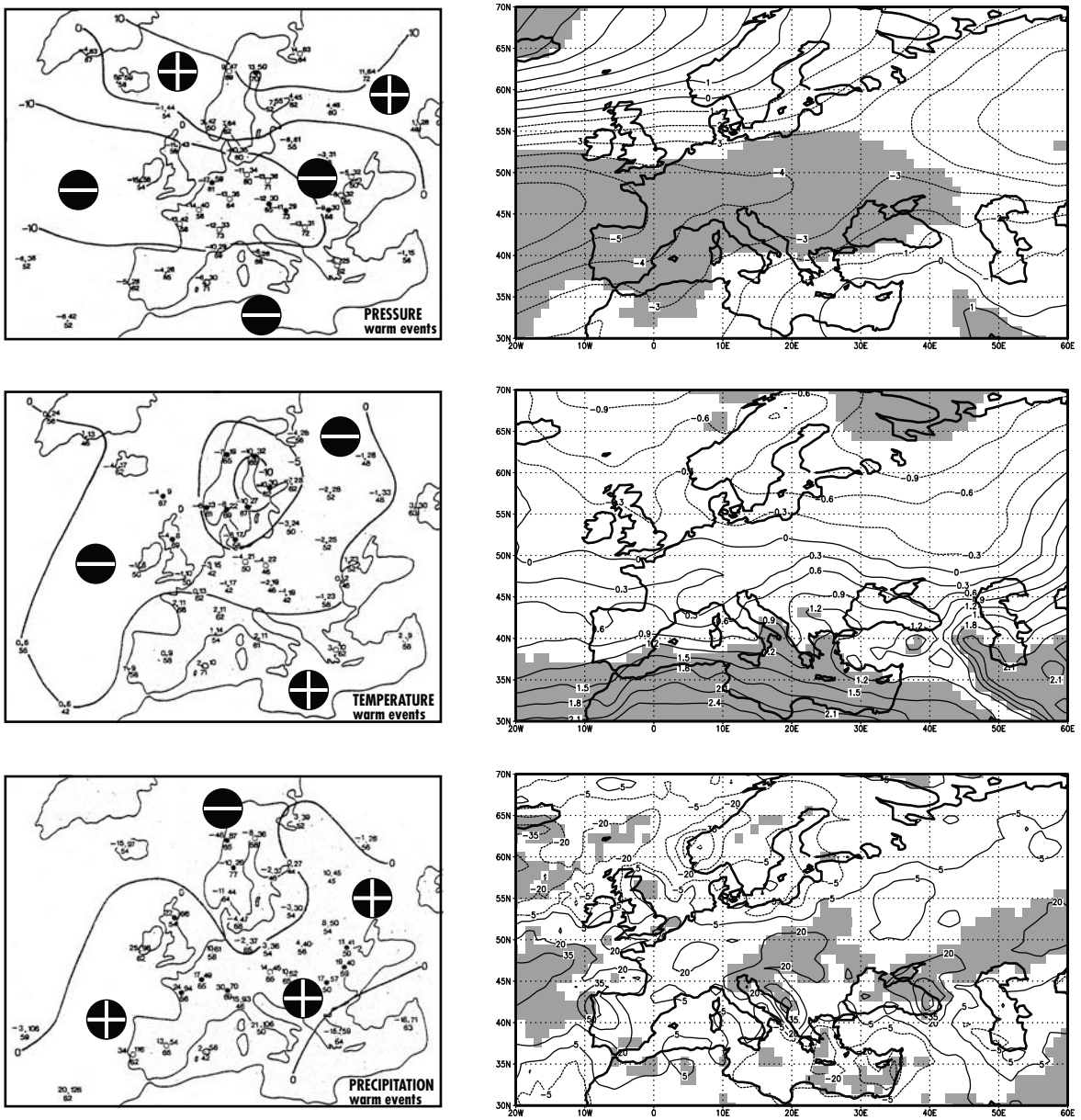

Fig.1: Right panels: Seasonal (DJF) ensemble mean response in the T106 experiment of SLP [hPa] (top), air temperature at 850 hPa [K] (middle), precipitation [mm/ month] (bottom). Shaded regions indicate significance on the 95% level according to a t-test. For comparison, the results of the composite study by Fraedrich and Müller (1992) are redrawn on the left (units: [1/10 hPa], [1/10 K], [mm/month], respectively; contour intervals: 1 hPa, 0.5 K, zero line only, respectively)

correspondence to the European La Niña composites by Fraedrich and Müller (1992). A more detailed analysis of these experiments is subject of current investigation.

References:

Bengtsson, L., K. Arpe, E. Roeckner, and U. Schulzweida, 1996: Climate predictability experiments with a general circulation model. *Climate Dynamics,* **12**, 261-278.

Ferranti, L., F. Molteni, and T.N. Palmer, 1994: Impact of localized tropical and extratropical SST anomalies in ensembles of seasonal GCM integrations. *Quart. J. Roy. Meteor. Soc*., **120**, 1613-1645.

Fraedrich, K., and K. Müller, 1992: Climate Anomalies in Europe Associated With ENSO Extremes. *Int. J. Climat.*, **12**, 25-31.

Mariotti, A., N. Zeng, and K.-M. Lau, 2002: Euro-Mediterranean rainfall and ENSO - a seasonally varying relationship. *Geophys. Res. Lett*., in press.

Merkel, U., and M. Latif, 2002: A High Resolution AGCM Study of the El Niño Impact on the North Atlantic/European Sector. *Geophys. Res. Lett*., in press.

Roeckner, E., K. Arpe, L. Bengtsson, M. Christoph, M. Claussen, L. Dümenil, M. Esch, M. Giorgetta, U. Schlese, and U. Schulzweida, 1996: The atmospheric general circulation model ECHAM-4: Model description and simulation of present-day climate. Max-Planck-Institut für Meteorologie, Hamburg, Report No. 218, 90 pp.

ENSO Related Precipitation Anomalies from the Tropics to the Extratropics

Scott Curtis[1,2] and Robert Adler[2]
[1]JCET / University of Maryland
Baltimore, MD, USA
curtis@agnes.gsfc.nasa.gov

[2]NASA / Goddard Space Flight Center
Greenbelt, MD, USA
adler@agnes.gsfc.nasa.gov

1. Introduction

Ever since the definition of the Southern Oscillation (SO) (Walker and Bliss, 1932) there have been earnest attempts to link interannual climate variations in the tropics with global precipitation anomalies (e.g. Rasmusson and Carpenter, 1983). Ropelewski and Halpert (1986, 1987) defined typical global and regional precipitation anomaly patterns during El Niño/Southern Oscillation (ENSO) episodes from 1877 to 1976. This work was expanded to include changes in the distribution of precipitation during ENSO (Ropelewski and Halpert, 1996). Furthermore, Mason and Goddard (2001) extended the RH analysis by using a high-resolution gridded data set over land for 1951 to 1996. However, for a truly global perspective on precipitation variations accompanying ENSO, one must rely on climate models (Smith and Ropelewski, 1997) or use satellite observations of precipitation. Satellite-gauge merged precipitation products have the advantage of being observationally-based, globally complete, and tied to surface measurements.

The Global Precipitation Climatology Project (GPCP), under the World Climate Research Program's (WCRP) Global Energy and Water Cycle Experiment (GEWEX), is tasked to produce high quality precipitation estimates from a combination of satellite sensors and gauge data for applications within the climate community. The monthly version 2 product is state-of-the-art, with a 2.5° spatial resolution and extending from 1979 to present (Adler et al., 2002). Although this period of satellite coverage is relatively short compared to the majority of gauge records, it is a period of strong and frequent ENSO events and thus useful for developing relationships between ENSO and global precipitation patterns. The GPCP version 2 data set has already been used to describe the role of precipitation during the 1997-1999 ENSO cycle (Curtis et al., 2001) and is used here to generalize ENSO-induced precipitation variability from the tropics to the extratropics.

2. Results

First, all months from January 1979 to September 2001 were sorted based on the ENSO Precipitation Index (ESPI). This measure of the strength of the anomalous precipitation gradient in the central Pacific (Curtis and Adler, 2000) is important for understanding global teleconnections, because precipitation releases latent heat in the atmosphere which drives the large-scale circulation. Normalized precipitation anomalies were averaged for the top third ESPI months (El Niño) and bottom third ESPI months (La Niña). The normalization process, dividing by the monthly standard deviation, highlights precipitation extremes in the mid- to high-latitudes that do not receive as much rainfall as the tropics.

The El Niño and La Niña composite maps (not shown) are near mirror images of each other and when combined (El Niño - La Niña) produce an ENSO signal with significant spatial continuity over large distances (Fig. 1, page 13). The canonical precipitation anomalies over land, described in previous studies (see section1), appear to be connected via the oceans in a horseshoe pattern. Enhanced precipitation extends from the central Pacific northward through the Southeastern U.S. to the North Atlantic and southward over the South Pacific to southern Chile. Reduced precipitation extends from the Maritime Continent northward over the North Pacific to Canada and southward past Australia and New Zealand and through the Drake Passage. Finally, enhanced precipitation extends from the horn of Africa northward to Central Asia. The southern counterpart appears to extend as far south as the Ross Sea via the Indian Ocean.

The teleconnections from the deep tropics to the high-latitudes are also seen with polar projections of the globe. Fig. 2a and b (page 13) are projections of Fig. 1 for the Northern and Southern hemisphere respectively. Positive precipitation anomalies dominate the Northern hemisphere poleward of 20° (Fig. 2a), except for the North Pacific, Canada, and Greenland as mentioned above. A banded structure to the anomalies is clearly seen in the Southern hemisphere (Fig. 2b), where there are fewer land masses to impede precipitation signals emanating from the tropics. Positive precipitation anomalies from the central Pacific and Indian Oceans and negative anomalies from the Maritime Continent spiral into Antarctica. This is consistent with a study by Sinclair et al. (1997) which showed a similar pattern in ECMWF mean sea level pressure and cyclone density anomalies during El Niño. Further work is needed to determine if the precipitation observations around Antarctica fit the dipole pattern described by Yuan (2001).

3. Summary

This preliminary study shows the usefulness of GPCP Version 2 data (Adler et al., 2002) in characterizing ENSO. Precipitation anomalies form global-scale horseshoe shapes opening to the east. The southern components of the horseshoes are stronger than the north-

ern components and appear to spiral into the South Pole. Thus, the teleconnection mechanism may act more efficiently over ocean than land.

While the GPCP data record is short compared to many gauge based data sets, there is good agreement between the satellite analysis and historical studies over land, such as Ropelewski and Halpert (1987). The high correlation over land as well as the global continuity of features gives us reasonable confidence in the analysis over the oceans. The obvious interaction between precipitation in the tropical Pacific and precipitation in the extratropics during ENSO deserves further study with global reanalysis products and GCM experiments.

References

Adler, R.F., G.J. Huffman, A. Chang, R. Ferraro, P. Xie, J. Janowiak, B. Rudolf, U. Schneider, S. Curtis, D. Bolvin, A. Gruber, J. Susskind, and P. Arkin, 2002: The version 2 Global Precipitation Climatology Project (GPCP) monthly precipitation analysis (1979-present). *J. Hydrometeor.*, submitted.

Curtis, S., and R.F. Adler, 2000: ENSO indices based on patterns of satellite derived precipitation. *J. Climate*, **13**, 2786-2793.

Curtis, S., R. Adler, G. Huffman, E. Nelkin, and D. Bolvin, 2001: Evolution of tropical and extratropical precipitation anomalies during the 1997-1999 ENSO cycle. *Int. J. Climatol.*, **21**, 961-971.

Mason, S.J., and L. Goddard, 2001: Probabilistic precipitation anomalies associated with ENSO. *Bull. Amer. Meteor. Soc.*, **82**, 619-638.

Rasmusson, E.M., and T.H. Carpenter, 1983: The relationship between eastern equatorial Pacific sea surface temperatures and rainfall over India and Sri Lanka. *Mon. Wea. Rev.*, **111**, 517-528.

Ropelewski, C.F., and M.S. Halpert, 1986: North American precipitation and temperature patterns associated with the El Niño/Southern Oscillation (ENSO). *Mon. Wea. Rev.*, **114**, 2352-2362.

Ropelewski, C.F., and M.S. Halpert, 1987: Global and regional scale precipitation patterns associated with the El Niño/Southern Oscillation. *Mon. Wea. Rev.*, **115**, 1606-1626.

Ropelewski, C.F., and M.S. Halpert, 1996: Quantifying Southern Oscillation-precipitation relationships. *J. Climate*, **9**, 1043-1059.

Sinclair, M.R., J.A. Renwick, and J.W. Kidson, 1997: Low-frequency variability of Southern Hemisphere sea level pressure and weather system activity. *Mon. Wea. Rev.*, **125**, 2531-2543.

Smith, T.M., and C.F. Ropelewski, 1997: Quantifying Southern Oscillation-Precipitation relationships from an atmospheric GCM. *J. Climate*, **10**, 2277-2284.

Walker, G.T., and E.W. Bliss, 1932: World Weather V. *Mem. Roy. Meteor. Soc.*, **4**, 53-84.

Yuan, X., 2001: An ENSO related climate pattern: the Antarctic dipole. *CLIVAR Exchanges*, **6** (4), International CLIVAR Project Office, Southampton, UK, 3-4.

CLIVAR Calendar

2002	Meeting	Location	Attendance
March 11-13	CLIVAR/ CliC Southern Ocean Panel, 1st Session	Hobart, Australia	Invitation
March 12-14	Intl. ARGO Science Team, 4th Session	Hobart, Australia	Invitation
March 13-16	CLIVAR VAMOS Panel, 5th Session	San Jose, Costa Rica	Invitation
March 18-23	Joint Scientific Committee of WCRP, 23th Session	Hobart, Australia	Invitation
May 6-8	WOCE/CLIVAR Working Group on Ocean Model Developm.	Hamburg, Germany	Invitation
April 22-26	European Geophysical Society, XXVII General Assembly	Nice, France	Open
May 22-25	CLIVAR Scientific Steering Group, 11th Session	Xi'an, China	Invitation
May 28-June 1	AGU Spring Meeting	Washington, USA	Open
June 13-15	International Symposium: En route to GODAE	Biarritz, France	Open
July 22-26	International TRMM Science Conference	Honolulu, Hawaii	Open
Nov. 18-22	Final WOCE Conference	San Antonio, USA	Open
Dec. 6-10	AGU Fall Meeting	San Francisco, USA	Open
2003	**Meeting**	**Location**	**Attendance**
Feb. 9-13	83rd AMS Annual Meeting	Long Beach, USA	Open
April 7-11	European Geophysical Society, XXVIII General Assembly	Nice, France	Open
2004	**Meeting**	**Location**	**Attendance**
June 21-25	First CLIVAR Open Science Conference	Baltimore, USA	Open

Check out our Calendar under: ***http://clivar-search.cms.udel.edu/calendar/default.htm*** *for additional information*

Weakening of the ENSO-Indian Monsoon Rainfall Relationship: The Indian Ocean Connection*

Karumuri Ashok[1,2] , Zhaoyong Guan[3] and Toshio Yamagata[4]
[1]Institute for Global Change Research
Yokohama City, Japan
ashok@jamstec.go.jp
[2]also at Indian Institute of Tropical Meteorology
Pune, India
[3]also at Nanjing Institute of Meteorology
Nanjing, China
[4]Also at Department of Earth & Planetary Science,
Graduate School of Science, University of Tokyo
Tokyo, Japan

We have investigated the influence of the recently discovered Indian Ocean Dipole (IOD; Saji et al., 1999) on the Indian summer monsoon rainfall (ISMR).

The correlation between the Indian Ocean Dipole Mode Index[1] (IODMI) and ISMR as 0.32, as found by Saji et al. (1999) who indicated that the relationship between the IOD and Indian Monsoon is not clear. However, of the 11 intense positive IOD events (anomalies more than one standard deviation) that occurred during 1958-1997, eight events (1961, 1963, 1967, 1977, 1983, 1993, 1994, and 1997; 73% of the positive IOD events during this period) correspond with the positive anomalies of the concurrent ISMR. Similarly, of the three negative IOD events during this 1958-1997, two events (1960 and 1992; 67% of the negative IOD events) correspond with negative anomalies of the ISMR. This observation, and the frequent occurrence of intense IOD events in the last decade, has prompted us to investigate whether the moving correlation between the IOD-ISMR changes from decade to decade and, in particular, its role in the weakening of the monsoon-ENSO correlation.

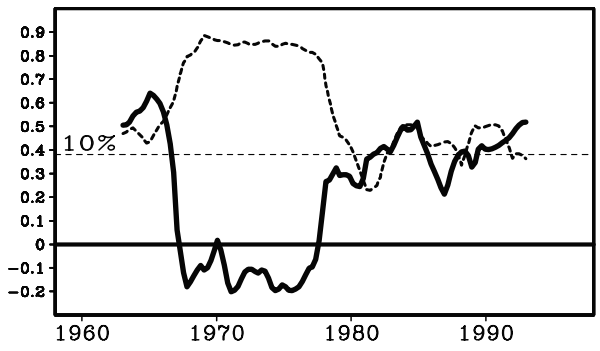

Fig. 1: The 41-month sliding correlation coefficients between ISMR and IODMI (solid), and those between monthly ISMR and NIÑO3 SST (dashed; to be multiplied by –1) during 1958-1997. The significant correlation value at 90% confidence level is 0.38 (verified by 1,000 randomized time series, using the Monte-Carlo simulations).

For this study, we used the ISMR data derived from the rain gauge in situ observations (Parthasarathy et al., 1995), and the GISST 2.3b dataset (Rayner et al., 1996). Both the rainfall and SST, from 1958-1997, have been subjected to 13-90 months band-pass filtering (Murakami, 1979). The ENSO signal has been removed from the SST of the Indian Ocean using the regression technique. This is necessary because of the co-occurrence of the positive/negative IOD and El Niño/La Niña events during some years.

The 41-month sliding correlation coefficients between the ISMR and the IODMI are presented in Fig. 1, along with those between the ISMR and NIÑO3 SST. The correlation coefficient between the IODMI and the ISMR is above 0.6 till about 1967, after which the correlation drops abruptly. In contrast, the negative correlation between the NIÑO3 SST and the ISMR is strengthened simultaneously from -0.45 to -0.85. Until around 1977 the IODMI has almost no correlation with the ISMR, whereas the ENSO strongly influences the ISMR during this period from 1967 through 1977. After this period, the ENSO-ISMR relation weakens, in agreement with previous studies (Krishna Kumar et al., 1999). By the late 1980s the correlation coefficient between the NIÑO3 and the ISMR weakens a lot. Meanwhile, the correlation between the IODMI and ISMR increases rapidly within a short period of about one year. Through the study period, the temporal evolutions of the correlations clearly complement each other. It is also evident that the IOD-ISMR correlation is currently on the rise. The high correlation observed in the early sixties can be attributed to intense IOD events during 1961, 1963, and 1967, which influenced the concurrent ISMR strongly. After that period, since there were not many strong IOD events till 1980s, the moving correlation values were very weak during this period. But the occurrence of intense IOD events in the 1980s and 1990s helped the correlation with the ISMR to rise.

When the ENSO occurs during the summer monsoon season, the correlation between the NIÑO3 SST and the ISMR is influenced by the IOD, depending on the phase and amplitude of the IODMI and NIÑO3 SSTA. When the IOD event occurs in the absence of an intense El Niño/La Niña, it can strongly influence the season's rainfall, as in 1961, and 1994. This is the reason why the

---

* This article is an extended abstract of our paper entitled "Impact of the Indian Ocean Dipole on the Relationship between the Indian Monsoon Rainfall and ENSO", which is in press in Geophysical Research Letters.

[1] the SST difference between the tropical western Indian Ocean (50°E-70°E, 10°S-10°N) and the tropical southeastern Indian Ocean (90°E-110°E, 10°S-equator).

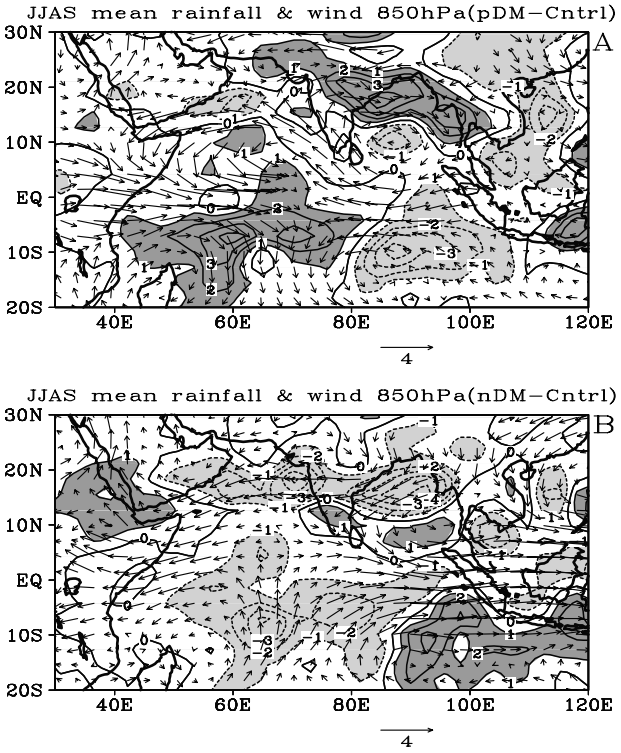

Fig. 2: The simulated ISMR difference (mm·day^{-1}) along with the corresponding difference in simulated 850 hPa winds (m·s^{-1}) (a) pDM-Cntrl (b) nDM-Cntrl; Cntrl is the control; experiment carried out with seasonally varying climatological SSTs. pDM denotes the experiment in which positive IOD anomaly has been imposed on climatological SST. NDM is similar experiment, but with negative IOD SSTA.

ENSO-ISMR relation changes and shows a complementary decadal variation with the ISMR-IOD relation, as shown in Fig. 1.

The presence of a positive IOD has facilitated normal or excess rainfall over the Indian region during the summers such as 1983, 1994, and 1997 despite the simultaneous occurrence of the negative phase of the Southern Oscillation (Behera et al., 1999, Webster et al., 1999). During JJAS in 1997, for example, the anomalous convergent flow in the lower troposphere is observed over the Bay of Bengal and the Indian subcontinent (Fig. 2a). The anomalous ENSO-induced subsidence over the Indian region that normally occurs during the 'ENSO only' years such as 1987 (Fig. 2b) is replaced by the IOD-induced convergence; this leads to the normal JJAS monsoon rainfall even during such strong El Niño years. On the other hand, during the years such as 1992, the prevailing negative IOD, and El Niño have co-operatively caused an anomalously deficit rainfall during the monsoon season. The ISMR anomalies also depend on the relative intensities of the IOD and the El Niño/La Niña events.

To understand how the IOD influences the ISMR, we have conducted three sensitivity experiments using an atmospheric general circulation model (AGCM) with full physics. Our results support the observations that the positive IOD causes anomalously surplus rainfall over the Indian region (Fig.2). The cross-equatorial winds from the southeastern tropical Indian Ocean intensify the summer monsoon circulation in the experiment conducted to study the positive IOD influence. The intensified convergence of winds coming from southeast causes anomalously surplus rainfall over the monsoon trough area. The conventional monsoon flow over the western Arabian Sea is anomalously weak, because of the anomalous circulation around the anomalously warm SSTA off the coast of East Africa. Near the west coast of Indian peninsula, however, this is compensated by the cross-equatorial wind from the anomalously cold SSTA prevailing to the west of Indonesia. The negative IOD has an opposite influence on the monsoon circulation and rainfall over India (Fig. 2b). The colder SST anomaly in the eastern tropical Indian Ocean causes reduction in convection during the positive DM event and hence the anomalous subsidence and divergence at the 850 hPa. Over the Bay of Bengal and monsoon trough area in the Indian region, on the other hand, convergence is induced in the lower troposphere, resulting in anomalously surplus rainfall (Fig. not shown). The atmospheric response to the IOD is baroclinic, and so the circulation at 200 hPa is opposite to those observed at 850 hpa (Fig. not shown).

It may be worthwhile to examine the possibility of using the IODMI for the climate prediction of the monsoon rainfall over India, in view of the recent increasing correlation between IODMI-ISMR (Fig.1).

References

Behera, S.K., R. Krishnan, and T. Yamagata, 1999: Unusual ocean-atmospheric conditions in the tropical Indian Ocean during 1994. *Geophys. Res. Lett*., **26**, 3001-3004.

Krishna Kumar, K.B. Rajagopalan, and M.A. Cane, 1999: on the weakening relationship between the Indian monsoon and ENSO. *Science*, **284**, 2156-2159.

Murakami, M., 1979: Large scale aspects of deep convective activity over the GATE area. *Mon. Wea. Rev.*, **107**, 994-1013.

Parthasarathy, B., A.A. Munot, and D.R. Kotawale, 1995: Monthly and seasonal rainfall series for all-India homogeneous regions and Meteorological sub-divisions: 1871-1994. Res.Rep. No. 65, Indian Institute of Tropical Meteorology, Pune, India.

Rayner, N.A., E.B. Horton, D.E. Parker, C.K. Folland, and R.B. Hackett, 1996: Version 2.2 of the Global sea-Ice and Sea Surface Temperature Data Set, 1903-1994. Climate Research Technical Note No. 74. Hadley Centre for Climate Prediction and Research, Meteorological Office, Bracknell, UK.

Saji, N.H., B.N. Goswami, P.N. Vinayachandran, and T. Yamagata, 1999: A dipole mode in the tropical Indian Ocean. *Nature*, **401**, 360-363.

Webster, P.J., A. Moore, J. Loschnigg, and M. Leban, 1999: Coupled ocean dynamics in the Indian Ocean during the 1997-1998. *Nature*, **401**, 356-360.

Subsurface interannual variability associated with the Indian Ocean Dipole

Suryachandra A. Rao[1], Swadhin K. Behera[1], Yukio Masumoto[1,2] and Toshio Yamagata[*1,2]
[1]Climate Variations Research Program, Institute for Global Change Research, Frontier Research System for Global Change, Yokohama, Japan.
[2]Department of Earth and Planetary Science, Graduate School of Science, University of Tokyo, Tokyo, Japan.
[*]Corresponding author: yamagata@eps.s-u.tokyo.ac.jp

1. Introduction

The subsurface variability in the tropical Pacific plays a crucial role in the evolution of the El Niño and Southern Oscillation (ENSO) (Neelin et al., 1998 and references therein). Existence of such a link in the tropical Indian Ocean (TIO), between the surface and subsurface interannual variability, is not very clear from the existing literature. Though several studies in the last decades discussed the variability of sea surface temperature (Saji et al., 1999; Webster et al., 1999; Iizuka et al., 2000 and references therein) there are only few studies that describe the subsurface variability (Tourre and White, 1995; Meyers, 1996; Murtugudde and Busalachi, 1999; Schiller et al., 2000).

Whether interannual variability in the subsurface Indian Ocean is dependent on the ENSO or not is not clear from the above studies. In light of the recent discovery of the Indian Ocean Dipole (IOD) in the TIO, and due to the availability of expanded satellite database and improved OGCM simulations, we reinvestigated the interannual variability in the subsurface TIO. We showed that, the significant interannual variability in the subsurface Indian Ocean is related to the IOD and not to the ENSO. Spatial patterns of this significant interannual variability show a dipole structure. Turnabout of the phase of this subsurface dipole, which gives rise to the quasi-biennial behavior of the TIO, is also discussed. The possible interactions between this subsurface dipole and the surface dipole are pursued. We addressed those issues by using three independent data sets, namely, satellite derived sea level data, in situ temperature profiles at selected locations, and simulation results from an OGCM. Complete details of our results are given in Rao et al. (2002).

2. Subsurface Dipole: Dominant mode of interannual variability in the TIO

The first EOF mode, which explains about 46% of the total variance of the TOPEX/POSEIDON sea level data, is shown in Fig. 1a (page 14). A dipole pattern is clearly seen in the TIO with positive loading in the east and negative loading in the west. The associated time series (Fig. 1c) coincides with two major positive IOD events; one in 1994 and the second one in 1997. We extended these results a bit more in time using the model simulated heat content anomalies. The first leading CEOF mode of the model heat content anomalies, which explains 39% of the total variance, also shows a dipole pattern (Fig. 1b). Further, time series of the first CEOF mode (Fig. 1c) shows strong negative peaks occurring in 1982, 1994 and 1997 coinciding with the positive IOD events. Note that all those IOD events that have occurred during the study period show a strong contribution to the predominant modes (also the second EOF/CEOF modes, see section 4). In contrast, the time series do not show any significant peaks during "pure ENSO", defined as the years during which no IOD events co-occurred in the Indian Ocean, like 1986/87 and 1991-93. Similar results are obtained using a long term (50 years) assimilated data of Carton et al. (2000). Therefore, the present results are robust irrespective of the time period selected for the analysis.

3. Influence of subsurface dipole on SST

Although the surface dipole vanishes by the end of the year during IOD events, its signature still remains in the subsurface owing to the large heat capacity of the oceans. To show how this subsurface phenomenon can affect the SSTA during subsequent months, we correlate sea level anomalies in the eastern Indian Ocean (10^oS - 10^oN; 90^oE-110^oE) with SSTA in the TIO at different lags by leading the SSTA. This exercise basically gives an outline of how a Rossby wave during its propagation to the west, can influence the SSTA in the basin. Such a correlation analysis is meaningful as we see propagating Rossby waves following IOD events. Positive correlation in the basin moves slowly to the west and reaches the western equatorial Indian Ocean after seven to eight months to change the polarity of the surface dipole (Fig. 2, page 14). Positive correlation reach maximum amplitude after twelve months probably due to the local seasonal upwelling along the west coast. The northwest and southeast slope of the positive/negative correlation in the southern TIO is another indication of the influence of Rossby waves on SSTA. This role of Rossby waves on the SSTA was not appreciated earlier in the TIO.

4. Quasi-biennial behavior of the TIO

We note here that the subsurface positive dipole event in the TIO is always followed by a negative dipole event as seen in Fig. 3 (page 14). This is because the downwelling Rossby waves from the eastern Indian Ocean prior to an IOD reach the western boundary by January/February in the following year and lift the sea level in the west. After reaching the western boundary, they reflect back into the equatorial waveguide as the

continued on page 17

From Curtis and Adler: ENSO Related Precipitation Anomalies from the Tropics to the Extratropics, page 8:

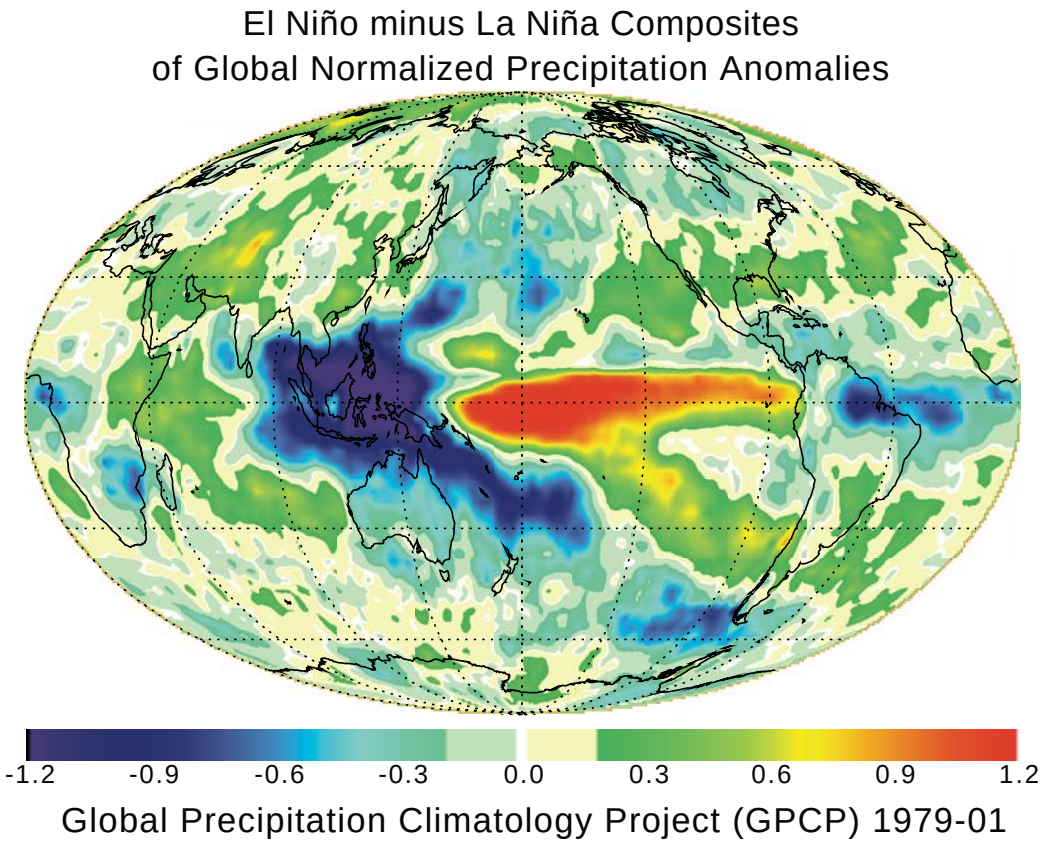

Fig. 1: Normalized precipitation departures associated with the ENSO Precipitation Index (ESPI) for January 1979 to September 2001. Map shows the difference between a composite of 91 El Niño months minus a composite of 91 La Niña months.

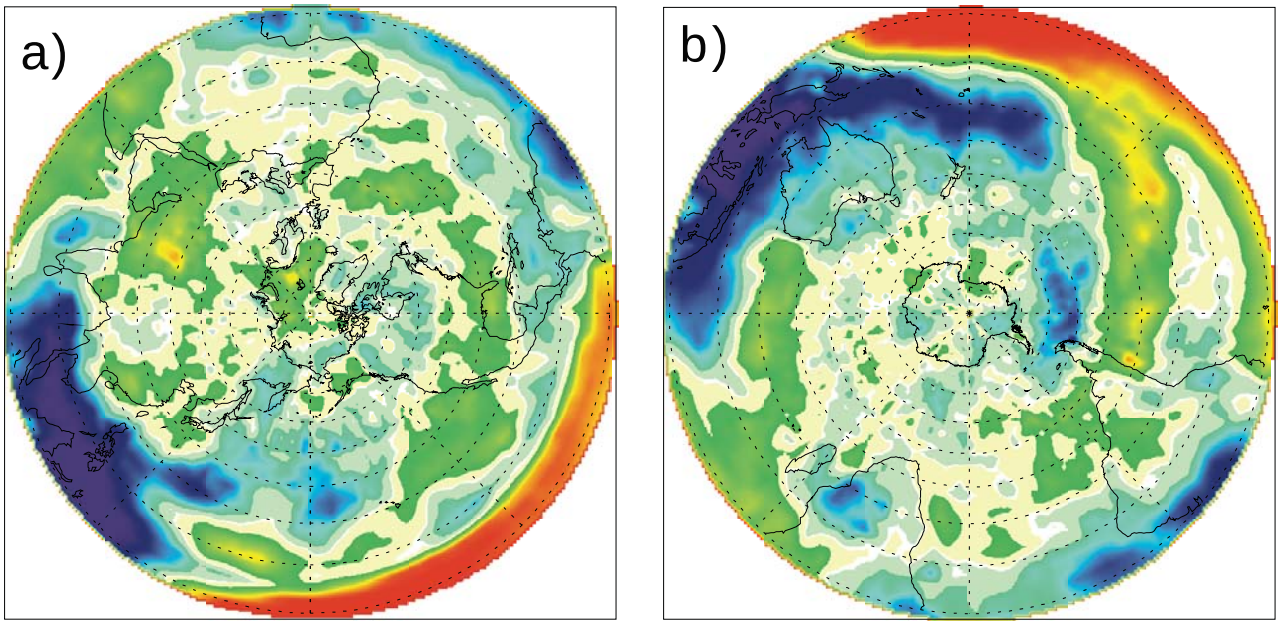

Fig. 2: Same as Figure 1 except for a) the Northern Hemisphere and b) the Southern Hemisphere.

From Rao et al.: Subsurface interannual variability associated with the Indian Ocean Dipole, page 12:

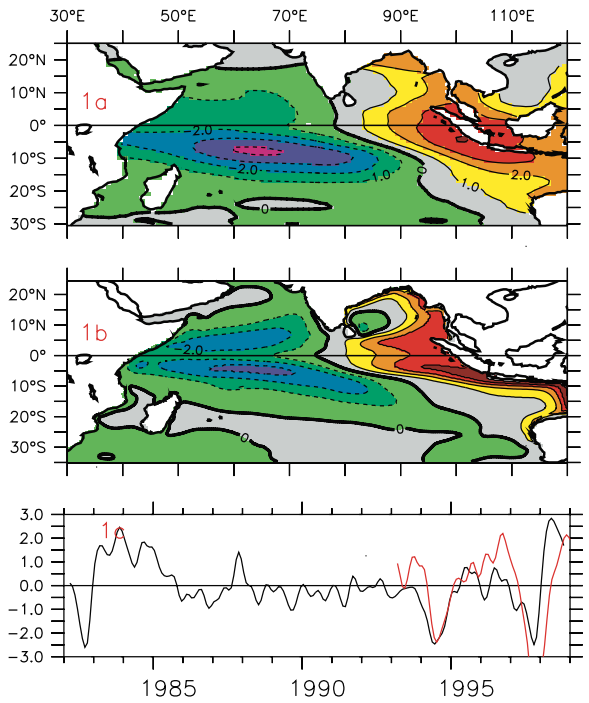

Fig. 1: (a) 1st EOF mode of TOPEX/POSEIDON sea level anomalies, (b) 1st CEOF (real) mode of model heat content anomalies, (c) principal components of sea level (red) and heat content (black) anomalies.

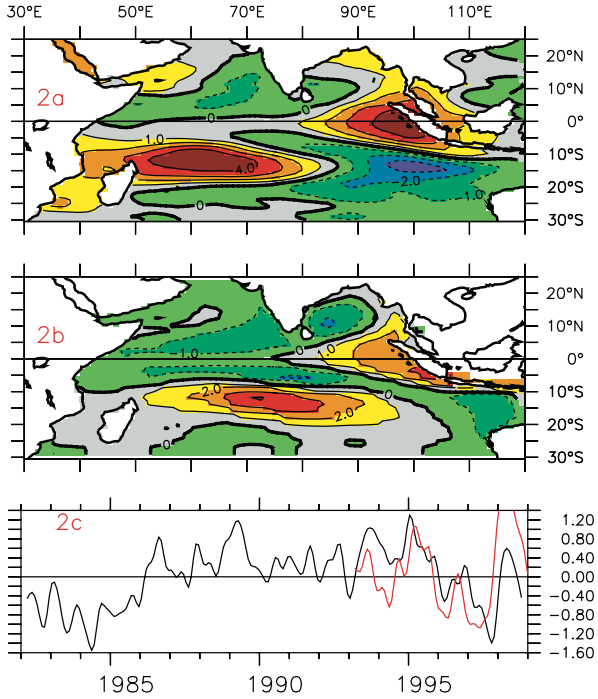

Fig. 2: (a) 2nd EOF mode of TOPEX/POSEIDON sea level anomalies, (b) 2nd CEOF (real) mode of model heat content anomalies, (c) principal components of sea level (red) and heat content (black) anomalies.

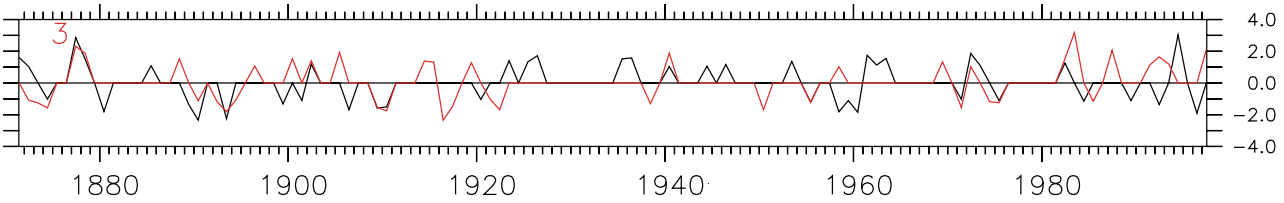

Fig. 3: Normalized annual mean Niño 3 SST anomalies (red) and dipole mode index (black). Values below one standard deviation are suppressed.

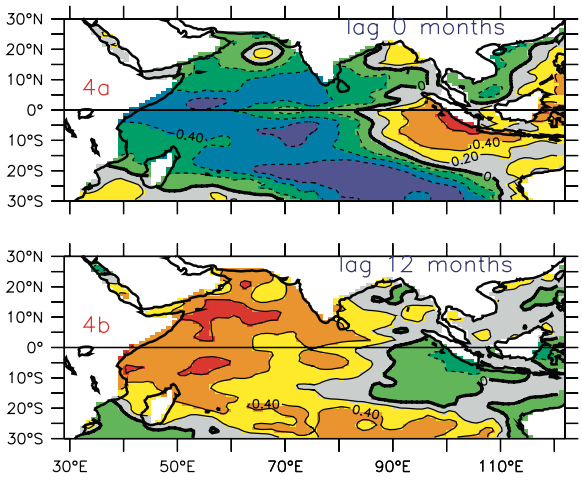

Fig. 4: Correlation coefficients between equatorial eastern Indian Ocean (90°E - 110°E; 10°S - 10°N) TOPEX/POSEIDON sea level anomalies and SST anomalies in the whole basin at (a) zero lag and (b) 12 months lag (sea level anomalies lag SST anomalies).

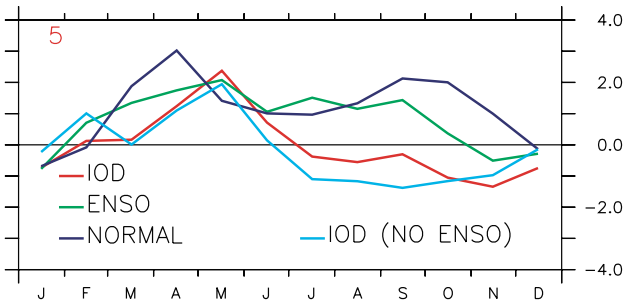

Fig. 5: Composite annual cycle of zonal winds (m s-1) in the equatorial Indian Ocean (70°E - 90°E; 5°S - 5°N) during different epochs.

From Lau et al.: The North Pacific Climate Regulator, page 22:

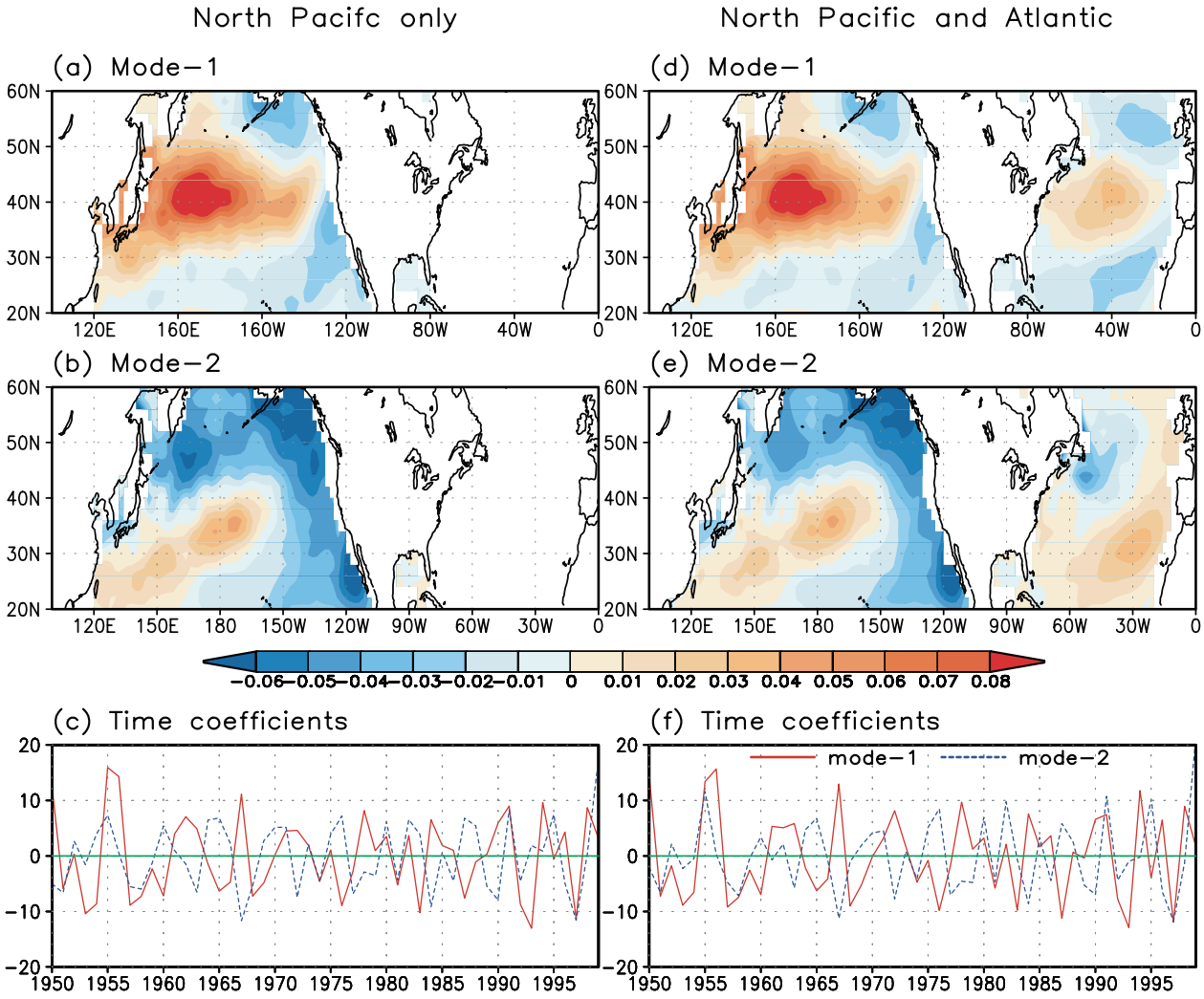

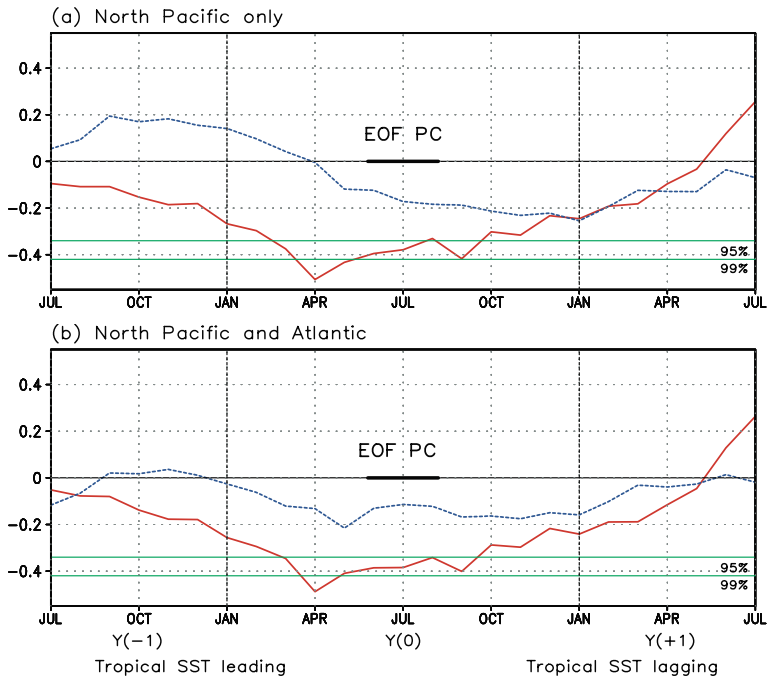

Fig. 1 (top panels): The EOF modes of interannual component of SST. (a)-(c) The first and second eigenvector components and the associated time coefficients in the North Pacific. (d)-(f) as in (a)-(c) except in the North Pacific and North Atlantic. Solid (red) and dashed (blue) lines of the time coefficients indicate the first and second mode, respectively. Multiplication of time coefficient and eigenvector gives unit of SST in °C.

Fig. 2 (left panels): Lagged correlation of the first and second principle components, denoted by solid (red) and dashed (blue) lines, respectively, with Nino 3.4 index (a) for the North Pacific only and (b) for the North Pacific and the North Atlantic. The correlation coefficients of 95% and 99% significant level are 0.34 and 0.42, respectively.

From Lau et al.: The North Pacific Climate Regulator, page 22:

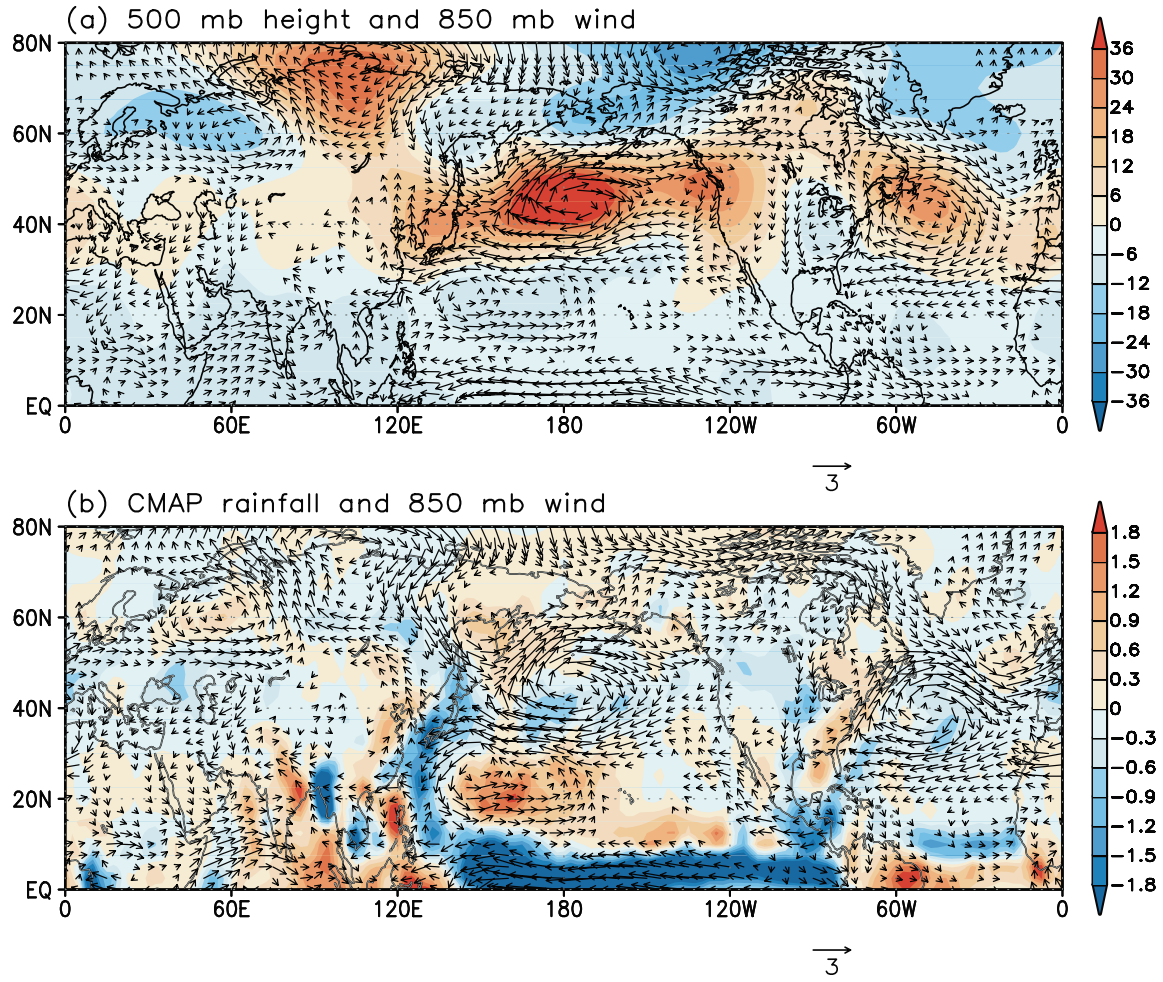

Fig. 3: Mode-1 composite of (a) 500 mb height (m) and 850 mb wind for the period 1950-1999, and (b) CMAP rainfall and 850 mb wind for the period 1979-99. Positive (negative) anomalies are shaded red (blue)

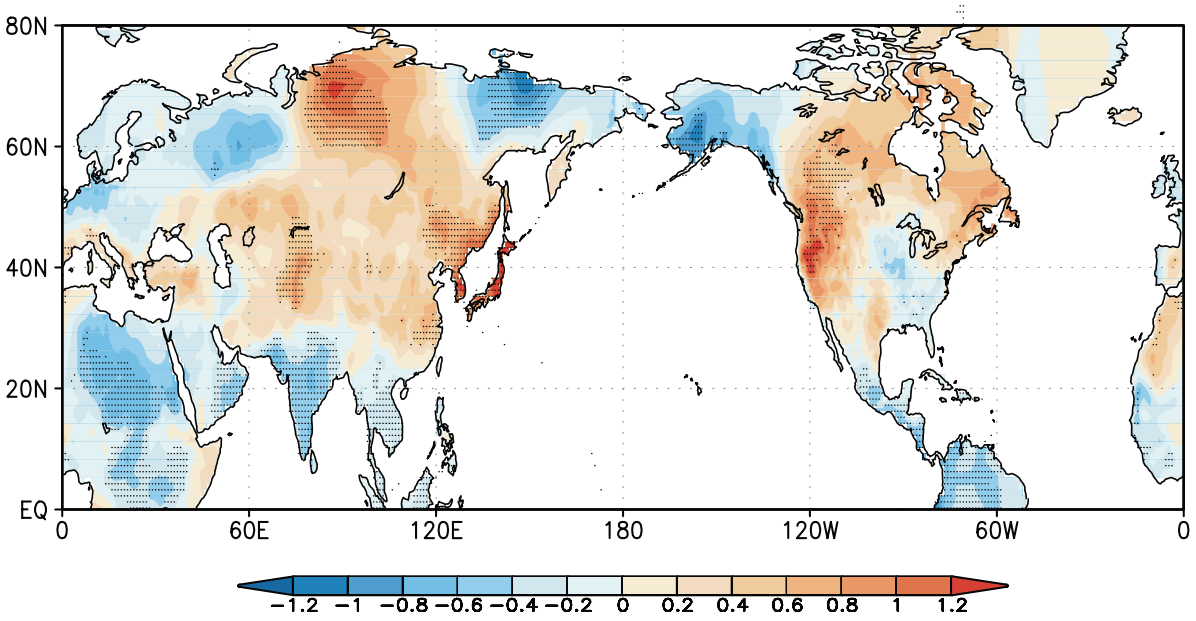

Fig. 4: Mode-1 composite of (a) CRU surface temperature (contour interval:0.3℃). (b) Surface temperature over the areas of correlation with mode-1 exceeding the 95% significant level is shaded.

continued from page 13

downwelling Kelvin wave. This downwelling Kelvin wave, upon reaching the eastern boundary, raises the sea level there. Moreover, since the reversal of zonal wind stress anomalies in the following February/March also excite a downwelling Kelvin wave, the sea level in the east rises further. The upwelling Rossby wave originated at the eastern boundary during the positive IOD events reaches subsequently the western boundary by April/May and depresses the sea level there. Local seasonal upwelling along the coast of Africa might further lower the sea level there when it is abnormally strong. These sequence of events give rise to the negative subsurface dipole in the equatorial Indian Ocean. This transformation of the positive subsurface dipole into the negative subsurface dipole may give rise to an interesting quasi-biennial behavior in the TIO; this quasi-biennial signal is found to be the second dominant mode of interannual variability in the TIO (Fig. 4). Therefore it is concluded that both the first and second dominant modes of the subsurface Indian Ocean are associated with the IOD.

5. ENSO vs IOD

The IOD is an internal coupled mode in the Indian Ocean, which at times co-occurs with the ENSO in the Pacific (Saji et al., 1999; Webster et al., 1999; Murtugudde et al., 2000; Iizuka et al., 2000). During the last 127 years, 14 (19) strong positive (negative) IOD events (defined as years during which annual mean of DMI exceeds one standard deviation) developed of which only 5 (7) events co-occurred during an ENSO event (Fig. 3). In other words 65% of the strong IOD events occurred when there was no ENSO in the tropical Pacific. This gives a clue that IOD can evolve independently many times and therefore considered as independent of ENSO.

Why "pure ENSO" influence is not seen in the subsurface TIO is an interesting question to raise at this point. Since the equatorial thermocline movement is mainly controlled by zonal winds, it is reasonable to expect that significant changes in the zonal winds occur only during the IOD events. As shown in Fig. 5, winds in the equatorial Indian Ocean change direction from July and continue to blow westward during the rest of the year during an IOD event. On the other hand, a significant change in the strength of zonal winds takes place only by October and lasts through November during a "pure ENSO event". Also the departures from the mean annual cycle during a "pure ENSO event", are small compared to that seen during the IOD events. The effect of the ENSO winds on the thermocline is only through the weakening of zonal wind stress. Thermocline variations associated with the IOD events are, however, much stronger owing to the complete reversal of zonal winds; the easterlies in the Indian Ocean favor upwelling at the equator. Associated with the shorter duration of wind anomalies during the pure ENSO, the subsurface variability is also short-lived, while the variability associated with IOD is long-lived. Therefore, the IOD influence is reflected in the EOF/CEOF analysis. The above interpretation does not change even after excluding the IOD events that co-occurred with El Niño events (Fig. 5). Even though, the IOD can develop as an internal coupled mode in the Indian Ocean , it may be related to the ENSO in some occasions through the atmospheric bridge, for example the 1997 event (Ueda and Matsumoto, 2000).

6. References

Carton, A. N., G. Chepurin, and B. Giese, 2000: A sinple ocean data assimilation analysis of the global upper ocean 1959-1995, part 1: Methodology. *J. Phys. Oceanogr.*, **30**, 294-309.

Iizuka, S., T. Matsuura, and T. Yamagata, 2000: The Indian Ocean SST dipole simulated in a coupled general circulation model. *Geophys. Res. Lett.*, **27**, 3369-3372.

Meyers, G., 1996. Variations of Indonesian throughflow and the El Niño - Southern Oscillation. *J. Geophys. Res.*, **101**, 12255-12263.

Murtugudde, R., and A.J. Busalacchi, 1999: Interannual variability in the dynamics and thermodynamics of the tropical Indian Ocean. *J. Climate*, **12**, 2300-2326.

Neelin, J.D., S.D. Battisti, A.C. Hirst, F.F. Jin, Y. Wakata, T. Yamagata, and S. Zebiak, 1998: ENSO theory. *J. Geophys. Res.*, **103**, 14261-14290.

Rao, S.A., S.K. Behera, Y. Masumoto, and T. Yamagata, 2002: Subsurface interannual variability in the tropical Indian Ocean with a special emphasis on Indian Ocean dipole. *Deep Sea Res. II*, in press.

Saji, N.H., B.N. Goswami, P.N. Vinayachandran, and T. Yamagata, 1999: A dipole mode in the tropical Indian Ocean. *Nature*, **401**, 360-363.

Schiller, A., J.S. Godfrey, P.C. McIntosh, G. Meyers, and R. Fielder, 2000: Interannual dynamics and thermodynamics of the Indo-Pacific oceans. *J. Phys. Oceanogr.*, **30**, 987-1012.

Tourre, Y.M., and W.B. White, 1995: ENSO signals in the global upper-ocean temperature. *J. Phys. Oceanogr.*, **25**, 1317-1332.

Ueda, H., and J. Matsumto, 2000: A possible trigerring process of east-west asymmetric anomalies, over the Indian Ocean in relation to 1997/98 El Niño. *J. Meteor. Soc. Japan*, **78**, 803-818.

Webster, P.J., A.M. Moore, J.P. Loschingg, and R.R. Leben, 1999: Coupled ocean-atmosphere dynamics in the Indian Ocean during 1997-98. *Nature*, **401**, 356-360.

Can the Arctic Oscillation impact the East Asian summer monsoon?

Dao-Yi Gong[1,2] and Chang-Hoi Ho[2]
[1]Key Lab of Environmental Change and Natural Disaster, Beijing Normal University, Beijing, China
gdy@pku.edu.cn
[2]Seoul National University, Seoul, Korea
hoch@cpl.snu.ac.kr

1. Introduction

This short note is summary of an article about the possible influence of Arctic Oscillation on the East Asian summer monsoon and monsoon rainfall we have recently finished.

In recent years there has been great interest in the Arctic Oscillation (AO) (Thompson and Wallace, 1998). Numerous studies have documented the strong influence of AO on the surface climate over the middle to high northern latitudes. These AO-related climate changes involve surface air temperature, precipitation, sea-ice over north polar and sub-polar regions, atmospheric circulation in lower troposphere including East Asian winter monsoon, Aleutian Low, Siberian High etc, and the extreme events including storms, cold waves and blocking activity (e.g., Thompson and Wallace, 2000, 2001; Gong et al., 2001; Boer et al., 2001).

However, these previous studies primarily focused on the simultaneous relationship, i.e., the AO's climate impacts in wintertime. Here we show evidence displaying the significant relationship between spring AO and East Asian summer monsoon and monsoon rainfall.

2. Data and method

AO indices are represented by the leading principal component time series of the monthly mean Northern Hemisphere (poleward 20ºN) sea level pressure field and available for period 1899-1999 (Thompson and Wallace, 1998). Six stations' rainfall data are selected. They are located over Yantgze River valley (east of 100ºE) and with seasonal rainfall record available for 1880 to 1999 (Wang et al., 2000). These six stations can represent the Mei-Yu rainfall features faithfully due to the high consistent variations of summer rainfall over this region as the empirical orthogonal function analysis revealed (Nitta and Hu, 1996). An historical monthly precipitation dataset for global land areas from 1900 to 1998 is also used here, which is gridded at a 5º latitude by 5º longitude resolution (Hulme, 1996). The 200hPa zonal wind data are taken from NCEP/NCAR reanalysis data sets for the period 1958-1999. Since there is strong interdecadal variability in summer monsoon and rainfall which is usually attributed to the tropical sea surface temperature anomalies (Weng et al., 1999; Hu, 1997), in order to remove the possible influence of this low-frequent changes and get a robust signals at inter-annual time scale, a high-pass 9-point Gaussian digital filter with the weights of 0.01, 0.05, 0.12, 0.20, 0.24, 0.20, 0.12, 0.05 and 0.01 is applied to all data. This filter removes the variations longer than 10 years and remains the inter-annual changes.

3. Results

It is widely recognized that the eastern Asian summer monsoon rainfall (Mei-Yu in China, Baiu in Japan or Changma in Korea) is most manifest along the Yangtze River valley and the southern Japan. On the inter-annual time scale, the long-term summer rainfall time series (six stations' mean, position see Figure 1) of Yangtze River valley are correlated to May AO index at a very high correlation coefficient of -0.39 during 1899-1999, significant at 99% confidence level. The AO signal in summer monsoon rainfall also shows zonal features over East Asia. Corresponding to one standard deviation stronger AO index there are about 20-40mm decreasing in summer rainfall over regions extending from Yangtze River valley to the southern Japan, and a 10-30mm increasing over the sorthern China. These changes are significant at 95% confidence level.

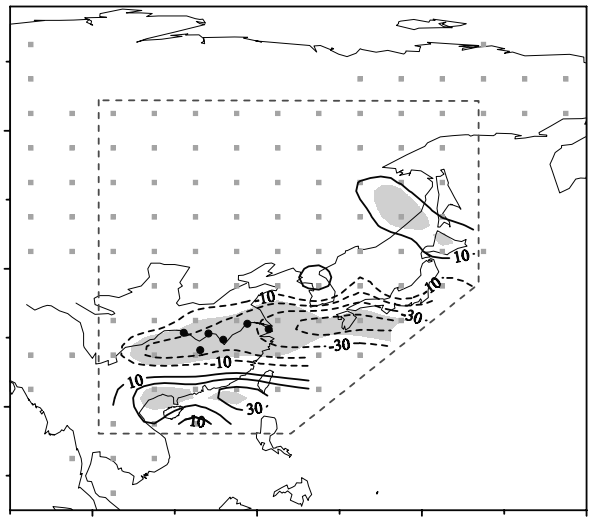

Fig. 1: Changes in summer precipitation (mm) corresponding to a one standard deviation of the May AO index. Computed over the period 1900-1998. All data are filtered to remove the low frequent variations, the first and last 4 years are discarded after filtering to avoid the edge effect. Grey squares indicate the grids with data availability above 95% in entire period. Regions above 95% confidence level shaded. Precipitation data are taken from Hulme (1992). Six stations along Yangtze River valley are also shown as filled circles (Wang et al., 2000). Contour interval is 10mm. Zero contours are omitted.

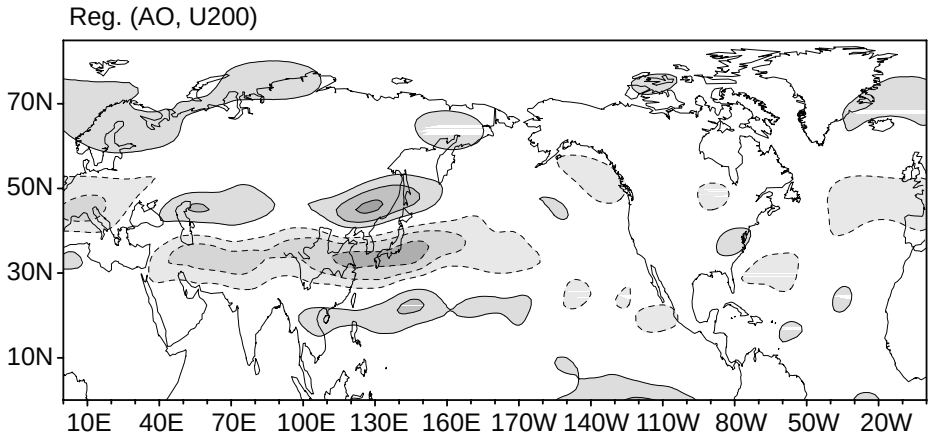

Fig. 2: Changes in summer zonal wind (m s^{-1}) at 200hPa associated with a one standard deviation anomaly in the May AO index. Prior to regression the AO time series are normalized. All data are filtered to remain only the inter-annual variation. Computed over the period 1958-1999. Zonal winds are taken from NCEP/NCAR reanalysis data. The contour interval is 0.5 m s^{-1} per standard deviation of May AO. Zero contours are omitted. Regions below –0.5 m s^{-1} and above +0.5 m s^{-1} are shaded.

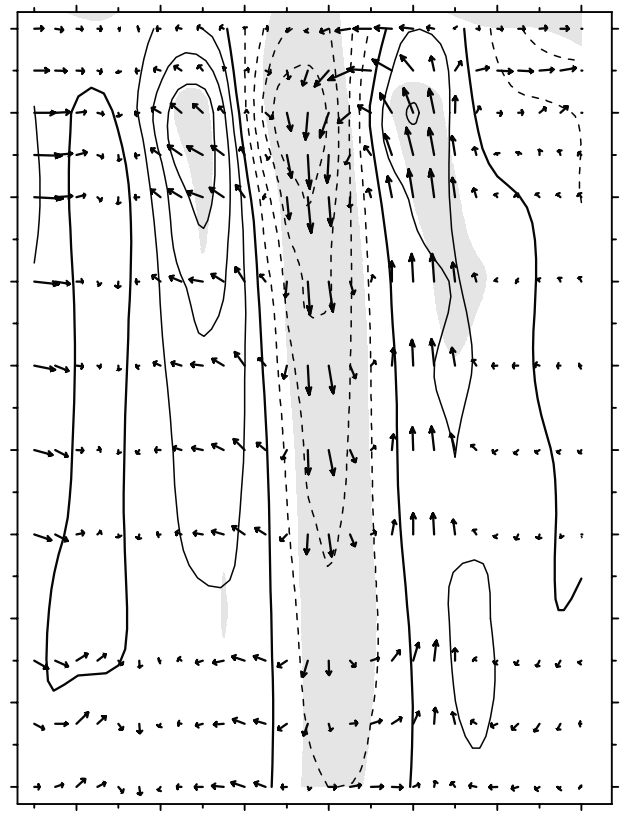

Fig. 3: Cross section of the zonal mean zonal wind (u), meridional wind (v) and vertical motion (ω) over East Asia (110°E-150°E) regressed onto the May AO index. The u is shown as the contours with interval of 0.3 m s^{-1}. Zero lines are bold, easterly are shown in dashed lines. Regions above 95% confidence level are shaded. The covariance of v and ω are shown as vectors. Values are m s^{-1} (for u and v) and hPa s^{-1} (for ω), corresponding to a one standard deviation anomaly in the May AO index. Before regression the AO index are normalized. The values of largest vectors are 0.47 m s^{-1} for v and 4.3 10^{-3}hPa s^{-1} for ω.

Two major large-scale circulation systems dominate the East Asia summer monsoon rainfall, one is the East Asian jet stream and the other is the western Pacific subtropical high (Liang and Wang, 1998). Previous studies indicated that the location of jet stream plays an important role in rainfall through direct and indirect circulation anomalies. It is found that the changes of summer 200hPa zonal wind are strongly related to the AO of May. Regression analysis shows that a pattern indicating a anomalous easterly around 30°N-35°N and a stronger zonal wind along 40°N-50°N in the East Asia is closely related to a higher positive mode of AO (Figure 2). This pattern is consistent very well with the relationship between summer monsoon rainfall and the East Asian jet stream.

The anomalous zonal wind, meridional and vertical wind in the boreal summer averaged over the domain of 110°E-150°E are regressed onto the May AO index (Figure 3). Results also display the well-defined features. Three cells are clearly described. Anomalous easterly with the concurrently strong descending motion are predominant around 30°N. The strong westerly to the north and the relatively weaker one to the south are also significant in the upper level, whereas the contours extend to the lower troposphere. The wind anomaly structure generally shows an equivalent barotropic vacillation with the largest covariance at ~200hPa. Evidently, the north-south displacement of the zonal wind jet appears at almost all pressure levels throughout troposphere.

All these consistent changes show that a stronger May AO is associated with a northwards movement of the summer jet stream, and a strong easterly as well as significant descending motion around 30°N. That gives rise to a drier condition in Yangtze River valley and a wetter anomaly over the southern China and far eastern Russia.

How can AO in spring impact the summer monsoon circulation? Some possible mechanism are suggested, including the jet-tropical sea surface temperature interaction (Lau et al., 2000), AO signal's downward propagation from the stratosphere (Baldwin and Dunkerton, 1999), wave-mean flow interaction, land surface process-atmosphere interaction (Yang and Lau, 1998). However, the responsible mechanisms are still open questions.

Acknowledgements

The first author is supported by the Natural Science Foundation of China (NSFC-40105007) and the National Key Developing Program for Basic Sciences (G1998040900). Grateful thanks are due to BK21 programme.

4. References

Baldwin, M.P., and T.J. Dunkerton, 1999: Propagation of the Arctic Oscillation from the stratosphere to the troposphere. *J. Geophys. Res.*, **104**, 30937-30946.

Boer, G.J., S. Fourest, and B. Yu, 2001: The signature of the annular modes in the moisture budget. *J. Climate*, **14**, 3655-3665.

Gong, D.Y., S.W. Wang, and J.H. Zhu, 2001: East Asian winter monsoon and Arctic Oscillation. *Geophys. Res. Lett*., **28**, 2073-2076.

Hu, Z.Z., 1997: Interdecadal variability of summer climate over East Asia and its association with 500hPa height and global sea surface temperature. *J. Geophys. Res*., **102** (D16), 19403-19412.

Hulme, M., 1992: A 1951-80 global land precipitation climatology for the evaluation of General Circulation Models. *Climate Dynamics*, **7**, 57-72. This dataset is gridded based on the station observations. Available at http://www.cru.uea.ac.uk.

Lau, K.M., K.M. Kim, and S. Yang, 2000: Dynamical and boundary forcing characteristics of regional components of the Asian summer monsoon. *J. Climate*, **13**, 2461-2482.

Liang, X.Z., and W.C. Wang, 1998: Association between China monsoon rainfall and tropospheric jets. *Q. J. R. Meteor. Soc*., **124**, 2597-2623.

Nitta, T., and Z.Z. Hu, 1996: Summer climate variability in China and its association with 500hPa height and tropical convection. *J. Meteor. Soc. Japan*, **74** (4), 425-445.

Thompson, D.W.J., and J.M. Wallace, 1998: The Arctic Oscillation signature in the wintertime geopotential height and temperature fields. *Geophys. Res. Lett*., **25**, 1297-1300.

Thompson, D.W.J., and J.M. Wallace, 2000: Annular modes in the extratropical circulation, Part I: Month-to-month variability. *J. Climate*, **13** (5), 1000-1016.

Thompson, D.W.J., and J.M. Wallace, 2001: Regional climate impacts of the Northern Hemisphere annular mode. *Science*, **293**, 85-89.

Wang, S., W.D.Y. Gong, J.L. Ye, and Z.H. Chen, 2000: Seasonal precipitation series over China since 1880. *Acta Geograph. Sinica*, **55** (3), 281-293. (In Chinese).

Weng, H.Y., K.M. Lau, and Y.K. Xue, 1999: Multi-scale summer rainfall variabiity over China and its long-term link to global sea surface temperature variability. *J. Meteor. Soc. Japan*, **77** (4), 845-857.

Yang S, and K.-M. Lau, 1998: Influence of sea surface temperature and ground wetness on Asian summer monsoon. *J. Climate*, **11**, 3230-3246.

Eighty-year oscillation of Summer Rainfall over North China and East Asian Summer Monsoon

Jinhong Zhu and Shaowu Wang
Department of Atmospheric Science,
School of Physics, Bejing University, Bejing, China
zjh@pku.edu.cn

1. Introduction

The East Asian Summer Monsoon (EASM) is one of the most important factors controlling summer rainfall over the eastern part of China. North China is a sensitive region to EASM and summer rainfall over North China is positively related to it. The subtropical high and Intertropical Convergence Zone (ITCZ) usually move northward much more than normal and North and South China have more precipitation when summer monsoon is stronger and more active, and vice versa. The anomaly of summer rainfall over North China was usually reverse to that over lower-middle Yangtze River valley (Wang et al., 1979). Although there were many studies on interannual variability of EASM and summer rainfall over the eastern part of China, interdecadal variability of this problem was less examined. Therefore, the long series of summer rainfall is analyzed to illustrate the 80yr-oscillation over the eastern part of China in this paper firstly. Then the relationship between summer rainfall and intensity of EASM on this time scale is examined. Finally, the variation of EASM is described according to summer rainfall over North China since 1470 and the possible mechanism is discussed.

2. Data

The rainfall data for 1470-1950 is taken from the 25 stations of history documents (Wang et al., 1981) and for 1951-1999 is used from 160 stations instrumentally measurements. All these data are converted into five coded levels and higher coded level represents drier weather (Wang et al., 1981). The sea level pressure (SLP) for 1873-1979 on 5° latitude by 10° longitude grid-point is obtained from Climatic Research Unit (CRU), at East Anglia University, UK (Basnett and Parker, 1997) and for 1948-1997 is from NCEP/NCAR Reanalyses.

3. Main findings

The correlation coefficients (CCs) are calculated between summer rainfall in Beijing and that over the eastern part of China using both the instrumentally observed rainfall data and the coded level data (not shown). These two CCs are highly correlated; moreover, both CCs show a significantly positive area over North China (near 35°-40°N and east of 110°E). Therefore, the long series of summer rainfall over North China can be represented by the coded level data of flood/drought in Beijing. The power spectrum analyses of 530yr rainfall coded level data on 25 stations demonstrate that 80yr-oscillation ex-

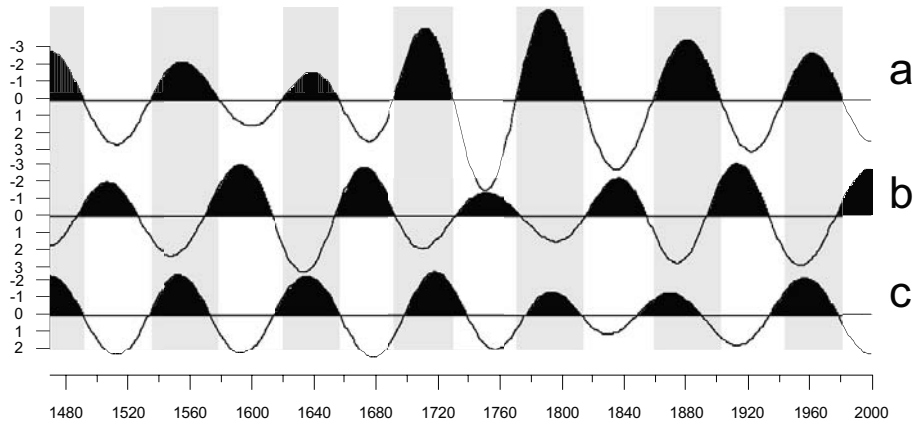

Fig. 1: The 80yr-oscillation component of summer rainfall over North China (a), lower-middle Yangtze River valley (b) and South China (c), the positive phases of summer rainfall anomalies are marked by diagonal lines and the periods of positive phase over North China are shaded.

ists in some areas and reaches 95% significant level. The 80yr-oscillation component of summer rainfall at North China even explains about 30% variance in low frequency band. Figure 1 shows that the phase of this component over North China is precisely consistent with that over South China (south of 25ºN and east of 110ºE) and out of phase to that along lower-middle Yangtze River valley (east of 110ºE near Yangtze River). Correlation coefficients of 80yr-oscillation component of summer rainfall between North China and the 25 stations distinctly illustrate the positive correlation between North and South China and negative correlation between North China and lower-middle Yangtze River valley (Fig. 2).

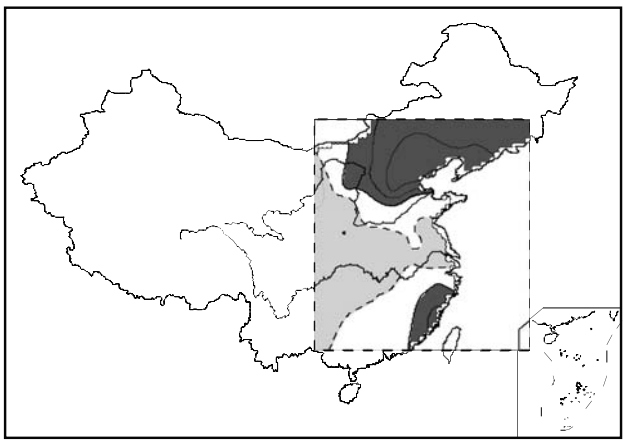

Fig. 2: The correlation coefficients' distribution of 80yr-oscillation component of rainfall grade data between North China and the eastern part of China for the period of 1470-1999. The positive CCs reached 95% significant level are in dark grey and negative CCs reached 95% significant level are light grey.

In this study, the interdecadal relationship between summer rainfall over North China and EASM are focus. Hence a new index of EASM is defined to describe the intensity of EASM associated with summer rainfall over North China. It is constructed by the followed procedure. Firstly, the correlation coefficient calculated between observed summer rainfall over North China and SLP in Northern Hemisphere for 1951-1997 is negative at region A (from 105º to 115ºE and from 30º to 35ºN) and positive at region B (from 120º to 130ºE and 20º to 25ºN). The magnitude of pressure difference between A and B represents the intensity of southwest wind between the two areas. Then, the index of EASM is computed using the averaged SLP at region A subtracted from that at region B. This index is composed of CRU data set for 1873-1979 and NCEP Reanalyses for 1980-1997 (Fig. 4b). The greater the index is, the stronger the southwest wind is and the much more northward EASM could reach. Although the index series is only 125yr, power spectrum analysis also indicates a significant 80yr-oscillation. For this component, summer rainfall is higher than normal over North China when this EASM index is higher and less when it is lower (Fig. 3).

The summer rainfall over North China during the past 530yr and the index of EASM during the past 125yr are showed in Fig. 4. For the period of 1873-1890 and 1950-1970, the index of EASM is relatively high and summer rainfall is also above normal over North China at the same time. From 1890 to 1950 and after 1970, this index is below normal and summer rainfall is less than normal, too. The correlation coefficient between summer rainfall over North China and this index during 1873-1997 is 0.19 reached 95%significant level. It is clearly shown in Fig. 4 that summer rainfall over North China is higher than normal during 1530-1580, 1620-1660, 1690-1730, 1770-1810, 1860-1900 and 1940-1980. Therefore, EASM might be stronger during the same periods if the EASM and rainfall relationship keeps unchanged. On the other hand, less summer rainfall could indicate weaker EASM in the other periods.

4. The possible relationship between EASM and solar activity

The above work shows the clear 80yr-oscillation in some areas over the eastern part of China. However, the mechanism of the EASM variation related closely to the anomalies of summer rainfall over the eastern part of China is still unclear. These anomalies of summer rainfall were averaged for 2.5 degrees latitude zones for the region covered by 25 stations and the decade running mean of the meridional-averaged anomalies was calculated for 1470-1979. The long spell of intensive flood was found over North China for six times during that period. The time interval between two flood spells was about 80 years. Furthermore, the 80yr cycle of rainfall

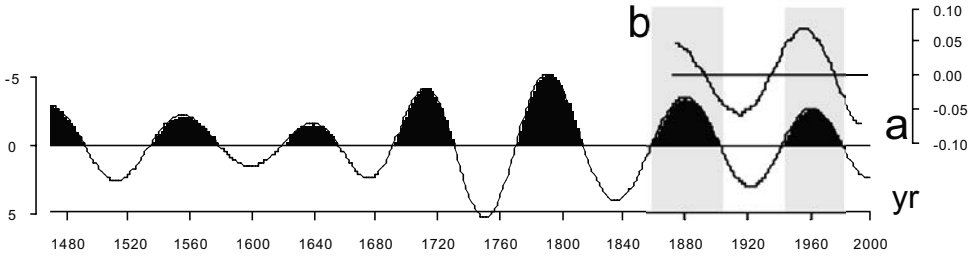

Fig. 3: The 80yr-oscillation component of summer rainfall over North China (line a) and the index of EASM (line b). The periods of positive phase of this component over North China are shaded.

over North China was related closely to 80yr cycle of solar activity by Wang et al. (1981). The similar work showed that this relationship is still remained after 1980 (Wang et al., 2000).

The climate variation along lower-middle Yangtze River valley related to solar-cycle was noticed by Hameed and Gong (1994). Many new results also illustrated that there is very close connection between EASM and solar activity (Hong et al., 1999, Shi et al., 1999, Zhou et al., 1999, Yao, 1999, Tang et al., 1999, An, 2000, Perry and Hsu, 2000). Therefore, it is possible that the intensity of EASM is modulated by the solar activity. However, the mechanism that EASM is affected by solar-cycle is still not clear and the further research is needed.

5. Summary and Discussion

A distinct 80yr-oscillation of summer rainfall is found over North China, lower-middle Yangtze River valley and South China. This oscillation over North China is in phase with that over South China and out of phase to that along lower-middle Yangtze River valley. Summer rainfall over North China correlates negatively with averaged SLP for the area near (105°-115°E and 30°-35°N), but positively with averaged SLP for the area near (120°-130°E and 20°-25°N). Therefore, an index of EASM is defined using the difference of averaged SLP over the above two regions. Summer rainfall over North China is greater than normal and drought occurs along lower-middle Yangtze River valley when strong EASM reaches North China. On the contrary, drought is found over North China and flood appears along lower-middle Yangtze River valley when EASM is close to normal or weak regime. Therefore, the EASM intensity could be inferred according to summer rainfall over North China since 1470.

The variation of summer rainfall over the eastern part of China is complicated. It is controlled by many factors and the relationships among those factors are even more complicated. However, the EASM is one of the most important factors controlling summer rainfall over the eastern part of China. The mechanism of 80yr-oscillation of summer monsoon is still not clear. Many studies suggested that EASM might be associated with solar activity. It needs to be proved by both diagnostics and GCM simulations.

References

An, Z., 2000: The history and variability of the East Asian paleomonsoon climate. *Quart. Sci. Rev.*, **19** (1-5), 171-187

Basnett, T.A., and D.E. Parker, 1997: Development of the Global Mean Sea Level Pressure Data Set GMSLP2, Climatic Research Technical Note No. 79, Hadley Centre, Meteorological Office, Bracknell, UK.

Hameed, S., and G. Gong, 1994: Variation of spring climate in lower-middle Yangtze River valley and its relation with solar-cycle length. *Geophys. Res. Lett.*, **21** (24), 2693-2696.

Hong, Y., D. Liu, H. Jiang, L. Zhou, J. Beer, B. Hong, Y. Zhu, H. Li, X. Leng, X. Qin, Y. Wang, Q. Lin, and Y. Zeng, 2000: Evidence for solar forcing of climate variation from $\delta^{18}O$ of peat cellulose. *Science in China*, *Ser. D*, **43** (2), 217-224.

Perry, C.A., and K.J. Hsu, 2000: Geophysical, archaeological, and historical evidence support a solar-output model for climate change. *PNAS*, **97** (23), 12433-12438.

Shi, Y., X. Liu, B. Li, and T. Yao, 1999: A very strong summer monsoon event during 30-40 kaBP in the Qinghai-

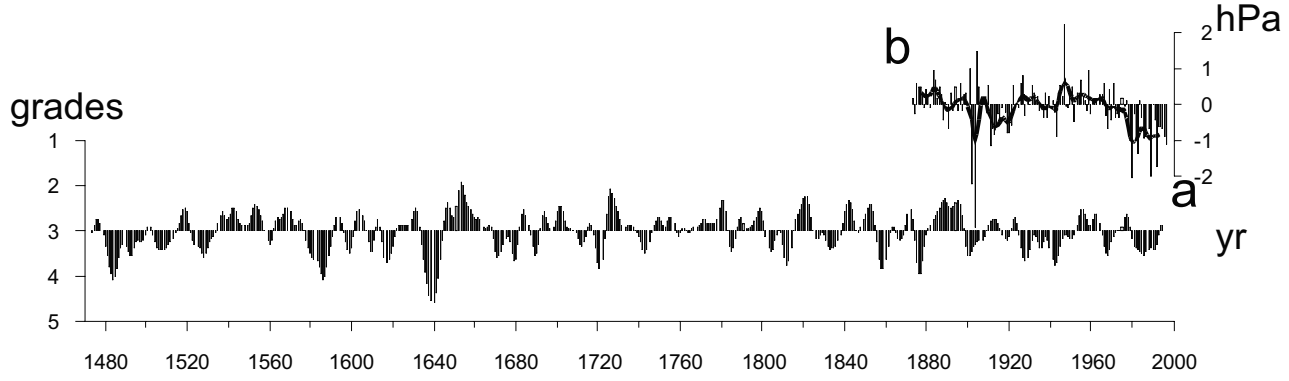

Fig. 4: The variation of the summer rainfall over North China after 1470 (line a) and the index of EASM after 1873 (line b). The solid line is Gauss-weighted filtered line of the EASM index.

Xizang (Tibet) Plateau and its relation to precessional cycle. *Chinese Science Bulletin*, **44** (20), 1851-1858.

Tang, L., C. Shen, K.-B. Liu, and J.T. Overpeck, 2000: Changes in South Asian monsoon: New high-resolution paleoclimatic records from Tibet, China. *Chinese Science Bulletin*, **45** (1), 87-91.

Wang, S., and Z. Zhao, 1979: Droughts and Floods in China 1470-1979. In: Wigley, T.M.L., M.J. Ingram, and G. Farmer, (eds.): *Climate and History*. Cambridge University Press, Cambridge, UK, 271-288.

Wang, S., Z. Zhao, and Z. Chen, 1981: Reconstruction of the Summer Rainfall Regime for the Last 500 Years in China. *GeoJournal*, **5** (2), 117-122.

Wang, S., and J. Zhu, 2000: The Interdecadal Variability of Summer Rainfall over East of China. *Climate Newsletter*, **2**, 20-27. (In Chinese)

Yao, T., 1999: Abrupt climatic changes on the Tibetan Plateau during the Last Ice Age—Comparative study of the Guliya ice core with the Greenland GRIP ice core. *Science in China*, **42** (4), 358-368.

Zhou, J., W. Zhou, H. Chen, X., Xue, and G. Nanson, 1999: Evidence for Asian summer monsoon precipitation instability of the Younger Dryas phase. *Chinese Science Bulletin*, **44** (9), 849-852.

The North Pacific Climate Regulator

William K. M. Lau[1], J.Y. Lee[2] and In-Sik Kang[2]
[1]Climate and Radiation Branch, Laboratory for Atmospheres, NASA/Goddard Space Flight Center, Greenbelt, MD, USA
lau@climate.gsfc.nasa.gov
[2]Department of Atmospheric Sciences, Seoul National University, Seoul, Korea

1. Introduction

Recently Lau and Weng (2000a; b; 2001) identified summertime teleconnection patterns linking variability in the East Asian monsoon to precipitation anomalies over the North American continent. In this note, we show evidence that the teleconnection patterns are manifestations of intrinsic summertime sea surface temperature (SST) modes of the North Pacific. These modes regulate climate variability of the Northern Hemisphere throughout the year, including the warm seasons and may provide sources of potential predictability on extratropical climate in addition to ENSO. This note focuses on the interannual climate regulation during the boreal summer.

2. Intrinsic modes of extratropical SST

Using NCEP SST data (Reynolds and Smith, 1994), we have computed EOF's of interannual (8 years> period> 1) year SST anomalies in the North Pacific basin. Figure 1 (page 15) shows the spatial patterns of the first two most dominant EOFs for June –July –August (JJA) which accounts for 25% and 19% of the interannual variance respectively. The first mode (Fig. 1a) features a basin-scale SST warm (cold) anomaly centered around 40°N, which is coupled to. cold (warm) SST anomalies in the Gulf of Alaska and in the subtropics off the west coast of the US. The second SST EOF shows major cold (warm) anomalies in the northern and eastern North Pacific, with concomitant warm (cold) anomalies in the western subtropical Pacific (Fig.1b). These SST patterns are similar to those obtained by Lau and Weng (2001) from regressions based on US summertime seasonal precipitation anomalies. EOF calculations with both North Pacific and North Atlantic show that the SST patterns (Fig. 1d, and e) and their principal components (Fig. 1c and f) are almost identical to those from North Pacific alone. In addition, the first combined EOF (Fig. 1d) shows that the North Pacific and North Atlantic SST have similar pattern suggesting that the extratropical oceans vary in phase, on interannual time scales. The structures of second EOF in the two oceans are also similar but appear to be 180° out of phase (Fig. 1e). Similar SST patterns to those shown in Fig. 1 can be obtained from regression against EOFs of North Atlantic alone (not shown). The analyses suggest that the North Pacific SST patterns shown in Fig. 1a and b are parts of a coherent global SST pattern linking the North Pacific *and* the North Atlantic The coherence in oceanic signals in the two ocean basins suggests the presence an "atmospheric bridge" linking them (Lau and Nath, 1996).

The lagged correlations of Nino3.4 SST with the principal components (PC) of the first and second SST EOF for the North Pacific and for the combined North Pacific and North Atlantic have been computed. It is clear that PC1 (Fig.2a, page 15) is correlated with Niño 3.4 SST (>95 % confidence level) for the current and previous spring. Yet it is not significantly correlated with Niño 3.4 SST in the previous or following winters, when the El Niño signals are strongest. The lagged correlation SST spatial patterns associated with PC1 (not shown) are distinctly different from the evolution of El Niño. For PC2, no significant correlation with Niño 3.4 SST exists at any lag. The principal components using combined North Pacific and Atlantic yields the same results (Fig. 2b). Hence it may be concluded that both extratropical SST modes are distinct from El Niño. The EOF1 patters may actually be influenced by El Niño evolution in the previous spring, but as the season progresses through the summer and fall, the EOF1 SST becomes increasing decoupled from the influence of tropical SST.

3. The atmospheric bridge

Using PC1 as the reference time series, we construct the composites of extreme events based on the 1-s threshold. Eleven events from the base record (1950—1999) are

selected for each phase and the composites are obtained as the difference between the positive (warm North Pacific) and the negative (cold North Pacific) events.

a. Circulation anomalies

Fig. 3a (page 16) shows the 850 hPa wind and 500hPa geopotential patterns associated with PC1. The most pronounced features are two zonally oriented low level anticylones occupying the entire North Pacific and the North Atlantic respectively. The anticyclones are associated with increased 500 mb geopotential height, which forms a cricum-global band along 40°N. Here, one gets the impression that the Pacific signal is a part of a global teleconnection pattern including large anomalies not only over the extratropical ocean but also over the polar land regions, and to a lesser degree the global tropics. The western end of the North Pacific anticyclone flow impinges on central and northeastern East Asia, and is coupled to a cyclonic circulation over the tropical western Pacific. The Atlantic anticyclone appears to have the similar impact over the northeastern North America. The geopotential height anomalies in the tropics have signs opposite from those in the midlatiudes, but have the same sign as the anomalies in the polar regions (>60°N), except over northern Siberia. The zonal structures over the western Pacific and East Asia can be identified with characteristic features of the East Asian monsoon (Lau et al., 2000). Overall, the global pattern suggests the presence of zonally symmetric structures in the global atmosphere-ocean, interrupted by land-ocean thermal contrasts in the northern hemisphere (Schubert et al., 2001).

b. Rainfall anomalies

To ensure the robustness of the teleconnection shown above, we have also used the last 21-year (1979-1999) to obtain composites of the 850mb wind and the CMAP rainfall, which is only available for this latter of the data period. Only 6 cases are selected for the composite shown in Fig. 2b. The basic large-scale features, especially the anticyclones over the North Pacific and the North Atlantic are similar to those shown in Fig. 2a. The anticyclone-cyclone coupling over the western Pacific is quite pronounced. Also obvious is the belt of negative rainfall anomaly connecting the southern flank of North Pacific anticyclone, the East China Sea, and the equatorial central and eastern Pacific. Over East Asia, below rainfall are found in Japan, southern Korea, above-normal rainfall in northern and northeastern China associated with the North Pacific anticyclone. The rainfall and circulation patterns suggest a westward shift of the western Pacific anticyclone, and a weakening of the *Mei-yu* (Baiu or Changmai) rain belt. Overall, above-normal rainfall is found over South Asia, including the Indian Ocean, except in the Bay of Bengal and Indo-China. The rainfall pattern in the Indo-Pacific region occur simultaneously with reduced rainfall over the equatorial central and eastern Pacific. Over North America, enhanced rainfall is found over the eastern and northeastern regions, but reduced rainfall over the Mid-west and western Canada, in conjunction with the establishment of the North Atlantic anticyclone anomaly. Since both the North Pacific and North Atlantic anticyclonic circulation overlain warm SST, it is conceivable that the extratropical SST anomalies are initially forced from the atmosphere, with the ocean warming up through reduced surface evaporation and increased surface solar radiation (Lau and Nath, 2001). Once the large scale SST anomaly pattern is set up, it is possible that it induces surface thermal contrasts which in turn drives the atmospheric circulation. In this way, the SST anomalies in the North Pacific and the North Atlantic, together with the continental heating may serve as anchors to the overlying atmospheric circulation.

c. Land surface temperature anomalies

The horizontal distribution of surface temperature anomalies associated PC1 (Fig. 4, page 16) shows that the North Pacific warmth is felt over extensive regions of Eurasia and North America except eastern Siberia, and Alaska, where below normal temperatures are found. Regions of positive temperature anomalies broadly coincide with regions of positive 500 mb height (see Fig. 3a) anomalies, indicating these are vertical extended hydrostatic anomalies. Interestingly, the land regions of the tropics, e.g., India, Indonesia, and northern South America also show below normal temperature, and they tend to coincide with regions of above-normal rainfall as can be seen in Fig. 3b. Over Asia, the warmest regions are concentrated over central and northern East Asia including Japan, with other warm areas over northern Siberia and central Asia. Over North America, the warmest region is the Pacific northwest and the entire Canada. The US Midwest and southwest is slightly cooler than normal, as are the land regions of central and northern South America.

3. Conclusion

Preliminary results show that the North Pacific Ocean plays a key role in regulating the summertime climate variability of Eurasia and North America. It is possible that the occurrence of large scale severe floods or droughts over these continents are strongly influenced by intrinsic coupled variability of the extratropical-ocean atmosphere. This coupled variability appears to be distinct, though not necessarily completely free, from tropical SST influence. Recently Lau et al. (2002) demonstrated that North Pacific SST anomalies can be utilized to enhanced potential predictability for summertime seasonal precipitation anomalies over the US northern Great Plains and the Midwest. Thus it is important that the North Pacific be further explored as a source of additional potential predictability for summertime climate variability of Eurasian and North America.

References

Lau, K.M. and H. Weng, 2000: Teleconnection linking summertime rainfall variability over North America and East Asia. *CLIVAR Exchanges*, **5**, 18-20.

Lau, K.M. and H. Weng, 2000: Remote forcing of US summertime droughts and floods by the Asian monsoon? *GEWEX News*, **10**, May Issue, 5-6.

Lau, K.M. and H. Weng, 2001: Recurrent teleconnnection patterns linking summertime precipitation variability over East Asia and North America. *J. Meteor. Soc. Japan*, submitted.

Lau, K.M., K.M. Kim, and S. Yang, 2000: Dynamical and Boundary Forcing Characteristics of regional components of the Asian summer monsoon. *J. Climate,* **13**, 2461-2482.

Lau, K.M., K.M. Kim and S. Shen, 2002: Canonical ensemble prediction of summertime seasonal precipitation over the United States. *Geophys. Res. Lett*., in press.

Lau, N. C., and M. J. Nath, 2001: Impact of ENSO on SST variability in the North Pacific and North Atlantic: seasonal dependence and role of extratropical air-sea interaction. *J. Climate,* **14**, 2846-2866.

Lau, N.C., and M.J. Nath, 1996: The role of "atmospheric bridge" in linking tropical Pacific ENSO events to extratropical SST anomalies. *J. Climate*, **9**, 2036-2057.

Reynolds, R., and T.M. Smith, 1994: Improved global sea surface temperature analysis using optimum interpolation. *J. Climate*, **7**, 929-948.

Schubert, S.D., M.J. Suarez, P.J. Pegion, and M.A. Kisler, 2002: Predictability of zonal means during boreal summer. *J. Climate*, accepted.

6th Session of the CLIVAR Working Group on Seasonal-to-Interannual Prediction

Andreas Villwock[1] and Steve Zebiak[2]
[1]International CLIVAR Project Office
c/o Institut für Meereskunde, Kiel, Germany
avillwock@ifm.uni-kiel.de
[2]International Research Institute, Palisades, USA
steve@iri.columbia.edu

Introduction

The 6th session of the CLIVAR Working Group on Seasonal-to-Interannual Prediction (WGSIP; previously known as CLIVAR NEG-1) was held at, at the Hungarian Meteorological Service, Budapest, Hungary, 5-7 November 2001. Dr. Sandor Szalai from the Hungarian Meteorological Service was the local host for the meeting. Dr. Steve Zebiak (Chairman of the WGSIP Panel) presided over the discussions.

During the three-day meeting there was extensive review of WGSIP research projects, discussions of plans for new initiatives, and other related international research activities.

A number of activities which had been initiated originally under the auspices of CLIVAR NEG-1 now have come to a conclusion. Reports of the ENSIP (ENSO Simulation Intercomparison Project) and the STOIC (Study of Tropical Oceans In Coupled models) project have recently been published in Climate Dynamics. Another study assessing the current status of ENSO forecast skill was also finalised in 2001 and published by the ICPO. Together with the Working Group on Couple Modelling, WGSIP organized a workshop on Decadal Predictability that was held in Scripps Institution of Oceanography, Oct. 4-6, 2000, The proceedings of the workshop were also published last year.

WGSIP activities

Recently, WGSIP has initiated a new activity on model experimentation and output standards. There were two main issues identified:

a) to define standards and
b) to agree upon methods to make the (meta)data available.

It was concluded from the discussion that WGSIP will determine an initial set of indices and diagnostic variables for a pilot phase. Issues such as definition of anomalies, specification of lead times, gridding, output formats at individual centres have to be included. In addition, the ICPO should explore options to develop a web-based interactive system for this purpose. WGSIP will interact with other WMO groups that have also been considering evaluation metrics for seasonal predictions.

Another ongoing activity of WGSIP is the Seasonal Prediction Model Intercomparison Project (SMIP). The follow on of the first phase, SMIP-2 is no under way for almost a year.

SMIP-2/HFP (historical forecast project) is a second component of SMIP-2 and aims to investigate the actual 1-season forecast skill that can be obtained using current model-based objective methods. Thus, SMIP-2/HFP compliments the standard SMIP-2 experiment which assesses the "potential" forecast skill that could be obtained if a perfect forecast of ocean and sea-ice conditions were available.

The specific objectives of SMIP-2/HPF are to:

- establish the "actual" 1-season forecast skill that is currently possible in a realistic operational, objective context

- provide a hindcast data set that has been produced with a uniform approach and which may be used to:
  - support the development and application of probability forecast methods including measures of reliability
  - encourage the further development and application of ensemble methods including super-ensemble approaches
- provide a benchmark against which to demonstrate improvement and to justify changes in operational 1-season forecast approaches and methods

Details of the experimental design for these experiments can be found under http://www-pcmdi.llnl.gov/smip. WGSIP encouraged interested group to participate.

A major focus of this WGSIP meeting was on downscaling and regional climate modelling. Dr. Hans v. Storch, director of the Institute for Coastal Research at the GKSS Research Center Geesthacht, Germany, gave a thoughtful and comprehensive review on the current status of regional modelling and downscaling in an invited presentation.

In addition, WGSIP welcomed the report of the ad-hoc Panel on Regional Climate Modelling and endorsed the idea of a workshop on regional climate modelling. As a potential future activity, the group will explore the possibilities for a tropical dynamical downscaling experiment ('big brother' experiment).The examples presented documented the powerful capabilities of present regional dynamical models. In this context, WGSIP welcomed the report of the ad-hoc Panel on Regional Climate Modelling and endorsed the idea of a workshop on regional climate modelling.

WGSIP was tasked by the CLIVAR Scientific Steering Group to provide guidance to basin panels and the CLIVAR Ocean Observations Panel OOP prior to end 2001 on priorities for

a. Real time observations in support of SIP
b. Delayed mode observations
c. Process studies. (WGSIP)

WGSIP asked a small group to draft such a statement which should be discussed and forwarded to the SSG subsequently.

Finally, most of the participants presented highlights of their current research efforts related to WGSIP. As multimodel ensemble techniques are of growing interest, the group considered to hold a scientific workshop to assess the current status of multimodel ensemble forecasting for seasonal prediction in the near future.

JSC/CLIVAR Working Group on Coupled Modelling - 5th Session -

Roger Newson[1] and Andreas Villwock[2]

[1]Joint Planning Staff for WCRP, WMO
Geneva, Switzerland
Newson_R@gateway.wmo.ch

[2]International CLIVAR Project Office
c/o Institut für Meereskunde, Kiel, Germany
avillwock@ifm.uni-kiel.de

The fifth session of the JSC/CLIVAR Working Group on Coupled Modelling (WGCM) was kindly hosted by the new Chair of the group, Dr. J. Mitchell, at his home institution, the Hadley Centre for Climate Prediction and Research, the Met Office, Bracknell, UK, from 4 to 7 February 2002. Participants were welcomed by the Chief Scientist of the Met Office, Dr. P. Mason (also Chair of the Steering Committee for the Global Climate Observing System, GCOS) and by Dr. J. Mitchell.

As customary at its sessions, WGCM reviewed recent relevant events and developments in the WCRP, including the recommendations pertaining to the group from the Joint Scientific Committee (JSC) for the WCRP and other modelling activities in the WCRP, such as those of the CLIVAR Working Group on Seasonal-to-Interannual Prediction, the CAS/JSC Working Group on Numerical Experimentation, the ACSYS/CliC Numerical Experimentation Group and in SPARC. A report was also given on the IGBP/IHDP/WCRP Global Change Open Science Conference: Challenges of a Changing Earth in Amsterdam, July 2001. This had emphasized that research into global change was becoming increasingly an interdisciplinary effort depending on all the core projects of WCRP, IGBP and IHDP. Thus, effective co-ordination between the three programmes, and their various sub-projects was of growing importance.

WGCM discussed a range of outstanding issues to be addressed in the development of coupled models, drawing from the list of uncertainties and priorities in the IPCC Third Assessment Report and from the experience of members. Among items stressed were:

- improved methods of quantifying uncertainties in climate projections and scenarios, including development and exploration of ensembles of climate simulations;
- increased understanding of the interaction between climate change and natural climate variability;
- the initialization of coupled models;
- the reduction of persistent systematic errors in cloud simulations, sea surface temperature etc.

- the variations in past climate as a tool in understanding the response to climate forcing factors;
- the reasons for different responses in different models;
- improved knowledge of cloud/climate forcing and the direct/indirect effect of aerosols (including refined methodologies for refining the analysis of feedback processes);
- improved simulation of regional climate and extreme events.

With specific regard to climate feedback, as noted in the IPCC Third Assessment Report, "the sign of net cloud feedback is still a matter of uncertainty, and various models exhibit a large spread." New approaches to this long-standing problem are needed, and, in particular, use of analysis methods that are conceptually linear are likely to be inadequate given the complex coupling of energy and water cycles in clouds. WGCM is thus joining with the GEWEX Radiation Panel in the organization of a workshop with the objectives of evaluating current methods for analysing feedbacks and results, identifying the main questions and issues, examining analysis methods from other disciplines and selecting new methods that could be investigated further for application in the climate area. At the same time, WGCM noted and encouraged other work aimed at evaluating cloud feedback, including improved methods of evaluating model clouds against satellite data, and techniques to separate dynamically and non-dynamically forced cloud changes that have picked out aspects of observed cloud variation which may be useful proxies for cloud feedbacks in a changed climate. WGCM is also continuing its climate sensitivity studies, now focussed on a systematic intercomparison of cloud feedbacks as simulated in models with ISCCP data, and in a slab ocean experiments (with 1 x CO_2 *and 2 x* CO_2*).*

The Coupled Model Intercomparison Project (CMIP) is one of the most important and long-standing initiatives of WGCM, having been started in 1995. There are now three components: CMIP1 to collect and document features of global coupled model simulations of present-day climate (control-runs); CMIP2 to document features of control runs and climate sensitivity experiments with CO_2 increasing at 1% per year; CMIP2+, as CMIP2, but all fields, all data, monthly means and some daily data are being collected. The range of extra fields at higher temporal resolution being assembled in CMIP2+ (compared to the limited fields, time-averaged blocks, monthly mean time series in CMIP1 and CMIP2) is enabling in-depth study of many additional aspects of coupled model simulations (e.g. feedback mechanisms, ocean processes, why different models have different responses, higher frequency phenomena). A complete list of the diagnostic sub-projects being undertaken can be consulted at **http://www-pcmdi.llnl.gov/cmip**. As well as the publication by individual authors of sub-project results, the IPCC Third Assessment Report drew substantially on several CMIP sub-projects, and included an analysis of CMIP models. A workshop to review results of CMIP is being planned for late in 2003. Subsequently, a new phase of CMIP, again in the form of a specified standard experiment, will be organized. This will be supplemented by separate co-ordinated "sensitivity" experiments, including in particular experiments designed to throw light on mechanisms which may play a part in ocean-atmosphere variability and predictability on decadal timescales.

Following up the increasing need for co-operation in global change research, WGCM is now working closely with the IGBP Global Analysis, Integration and Modelling (GAIM) element of IGBP, including especially the planning of the "Coupled Carbon Cycle Climate Model Intercomparison Project" (C4MIP). In the first phase, interested groups are being invited to undertake a historical land-atmosphere experiment with global models having full coupling between radiation, biogeochemical cycles and carbon dioxide with specified sea surface temperature forcing, carbon dioxide emissions, and land-use change. Key diagnostics will include the model-predicted carbon dioxide fluxes and concentrations. Growing interactions between WGCM and GAIM are foreseen in the task of developing the comprehensive Earth system models that will be needed. To this end, it is hoped that the next session of the two groups will be held jointly and that, in 2003, a joint workshop on Earth system modelling will be held.

The report of the joint WGNE/WGCM ad hoc panel on regional climate modelling was presented to the session. It was recognized that dynamical atmospheric regional climate models have matured over the past decade and are used in a wide spectrum of applications. The process of improving the models should be guided by the needs of specific applications. The sensitivity of regional climate model simulations to computational domain size, to the jump in resolution between the nesting data and the regional climate model, and to errors and deficiencies in nesting data required further investigation. Above all, it was reiterated that the final quality of the results of a regional climate model depended fundamentally on the realism of the large scales simulated by the driving general circulation model. WGCM welcomed the report but stressed the importance of assessing the added value provided by a regional climate model compared with a statistical down-scaling approach. WGCM endorsed proposals made for an international regional climate modelling workshop (probably in 2003), and plans for a "Regional (climate) Model Intercomparison Project" (analogous to AMIP and CMIP). It was stressed that tests with reanalyses should also be undertaken to verify the ability of regional climate models to simulate the present climate.

**Are you looking for the CLIVAR Calendar?
In this issue you will find CLIVAR meetings on page 9.**

Contents

In this issue

The CLIVAR Newsletter Exchanges is published by the International CLIVAR Project Office.

ISSN No.: 1026 - 0471

Editors: Andreas Villwock and John Gould

Layout: Andreas Villwock

Printed by: Technart Ltd., Southern Road, Southampton SO15 1HG, UK.

Production supported with funding from the Japan Marine Science and Technology Center (JAMSTEC).

CLIVAR Exchanges is distributed free-of-charge upon request (icpo@soc.soton.ac.uk).

If undelivered please return to:

International CLIVAR Project Office
Southampton Oceanography Centre, Empress Dock, Southampton, SO14 3ZH, United Kingdom